

Galilean-Invariant XEFT

Eric Braaten

*Department of Physics, The Ohio State University,
Columbus, OH 43210, USA*

(Dated: March 17, 2015)

XEFT is a low-energy effective field theory for charm mesons and pions that provides a systematically improvable description of the $X(3872)$ resonance. A Galilean-invariant formulation of XEFT is introduced to exploit the fact that mass is very nearly conserved in the transition $D^{*0} \rightarrow D^0\pi^0$. The transitions $D^{*0} \rightarrow D^0\pi^0$ and $X \rightarrow D^0\bar{D}^0\pi^0$ are described explicitly in XEFT. The effects of the decay $D^{*0} \rightarrow D^0\gamma$ and of short-distance decay modes of the $X(3872)$, such as $J/\psi\pi^+\pi^-$, can be taken into account by using complex on-shell renormalization schemes for the D^{*0} propagator and for the $D^{*0}\bar{D}^0$ propagator in which the positions of their complex poles are specified. Galilean-invariant XEFT is used to calculate the $D^{*0}\bar{D}^0$ scattering length to next-to-leading order. Galilean invariance ensures the cancellation of ultraviolet divergences without the need for truncating an expansion in powers of the ratio of the pion and charm meson masses.

PACS numbers: 14.40.Rt, 14.40.Lb

I. INTRODUCTION

The surprising discovery of the $X(3872)$ by the Belle Collaboration in 2003 [1] marked the beginning of a renaissance in quarkonium spectroscopy [2]. Dozens of new mesons whose constituents include a heavy quark and antiquark and with mass above the open-heavy flavor threshold have been observed. They are collectively referred to as XYZ mesons. Some of the XYZ mesons are electrically charged and therefore must be tetraquark mesons whose constituents also include a light quark and antiquark. The pattern of the observed XYZ mesons remains unexplained. In particular, the relation between the $X(3872)$ and the other XYZ mesons is still not understood.

The discovery decay mode $J/\psi\pi^+\pi^-$ of the $X(3872)$ implies that its constituents must include a charm quark and antiquark. However the $X(3872)$ has properties inconsistent with conventional charmonium, including comparable branching fractions into decay modes with isospin 0 and isospin 1. The J^{PC} quantum numbers of the $X(3872)$ were finally established by the LHCb Collaboration in 2013 to be 1^{++} [3]. Its mass is extremely close to the threshold for the pair of charm mesons $D^{*0}\bar{D}^0$. By combining precise measurements of the mass M_X of the $X(3872)$ in the $J/\psi\pi^+\pi^-$ channel with precise measurements of the masses M_* and M of the D^{*0} and D^0 , the difference δ_X between the $D^{*0}\bar{D}^0$ threshold and the mass has been determined to be

$$\delta_X \equiv (M_* + M) - M_X = 0.11 \pm 0.23 \text{ MeV}. \quad (1)$$

The quantum numbers 1^{++} of the $X(3872)$ imply that it has an S-wave coupling to the charm meson pairs $D^{*0}\bar{D}^0$ and $D^0\bar{D}^{*0}$. Given the small value of δ_X , the universality of near-threshold S-wave resonances implies that the $X(3872)$ must be a bound state (if $\delta_X > 0$) or a virtual state (if $\delta_X < 0$) whose constituents are the $C = +$ superposition $D^{*0}\bar{D}^0 + D^0\bar{D}^{*0}$ [4]. The observation of $X(3872)$ in hadron collisions strongly suggests that it is a bound state (like the deuteron) rather than a virtual state (like the dineutron). One universal property of S-wave near-threshold bound states is that the mean separation $\langle r \rangle_X$ of the constituents is determined by the binding energy δ_X : $\langle r \rangle_X = (8\mu\delta_X)^{1/2}$, where μ is the reduced mass of $D^{*0}\bar{D}^0$ [5]. Given the binding energy $\delta_X = 0.11_{+0.23}^{-0.11}$ MeV, the mean separation of the charm mesons is predicted to be $6.8_{-3.9}^{+8.0}$ fm. Thus the size of the $X(3872)$ is comparable to that of the largest nuclei.

The universal properties of S-wave near-threshold bound states imply that most of the probability of the $X(3872)$ is in a molecular component consisting of well-separated charm mesons $D^{*0}\bar{D}^0$. (From now on, the equally probable $D^0\bar{D}^{*0}$ component will usually not be mentioned explicitly.) At short distances, the wavefunction of the $X(3872)$ can have other components with smaller probabilities. One possible component is the 1^{++} P-wave charmonium state $\chi_{c1}(2P)$, whose constituents are $c\bar{c}$. Another possibility is an isospin-0 tetraquark with constituents $cq\bar{c}\bar{q}$, where q is a light u or d quark. It could be a compact tetraquark, it could have substructure consisting of the diquark clusters cq and $\bar{c}\bar{q}$, or it could have substructure consisting of color-singlet clusters, such as the pair of mesons $J/\psi\omega$. There are also hexaquark components of the wavefunction with constituents $cqq\bar{c}\bar{q}\bar{q}$. One such component that is particularly important is $D^0\bar{D}^0\pi^0$, because the constituent D^{*0} in the dominant component of the wavefunction can decay into $D^0\pi^0$. In considering the various possible components of the $X(3872)$ wavefunction, it is essential to take into account their couplings to $D^{*0}\bar{D}^0$ and the resonant interactions between the charm mesons.

The interplay between the $D^{*0}\bar{D}^0$, $D^0\bar{D}^0\pi^0$, and other components of the wavefunction can be treated systematically using an effective field theory in which the D^{*0} , \bar{D}^0 , and π^0 are explicit degrees of freedom. Such an effective field theory has been developed by Fleming, Kusunoki, Mehen, and van Kolck and named XEFT [6]. In its simplest form, XEFT is a nonrelativistic field theory for D^{*0} and D^0 , their antiparticles, and π^0 . It is straightforward to extend XEFT to include the charged charm mesons and the charged pions. In XEFT, the interactions between D^{*0} and \bar{D}^0 must be treated nonperturbatively in order to generate a bound state that can be identified with the $X(3872)$. Fleming et al. showed that pion-exchange interactions can be treated perturbatively along with the range corrections to $D^*\bar{D}$ interactions [6]. We denote the masses of D^{*0} , D^0 , and π^0 by M_* , M , and m , respectively. We denote the difference between the D^{*0} mass and the sum of the D^0 and π^0 masses by δ :

$$\delta \equiv M_* - (M + m) \approx 7.14 \pm 0.07 \text{ MeV.} \quad (2)$$

The power counting of XEFT is defined by taking external momenta, the binding momentum scale $\sqrt{M\delta_X}$ of the $X(3872)$, and the momentum scale $\sqrt{m\delta}$ of the pion to all be low momentum scales of order Q . The low energy scales include the binding energy δ_X of the $X(3872)$, the kinetic energy scale δ for a pion, and the kinetic energy scale $m\delta/M$ for a charm meson. The high momentum or energy scales include m , M , and $4\pi f_\pi$, where f_π is the pion decay constant. Amplitudes are calculated as systematic expansions in powers of Q divided by a high momentum or energy scale. In the original paper on XEFT by Fleming et al., the momentum distributions in the decay of $X(3872)$ to $D^0\bar{D}^0\pi^0$ were calculated to next-to-leading order (NLO) in the XEFT power counting and to leading order in an expansion in powers of m/M [6].

There have been a number of subsequent applications of XEFT. Fleming and Mehen applied XEFT at leading order (LO) to decays of the $X = X(3872)$ into the P-wave charmonium state χ_{cJ} plus one or two pions [7, 8]. Mehen and Springer applied XEFT at LO to the radiative decays $X \rightarrow \psi(2S)\gamma$ and $\psi(4040) \rightarrow X\gamma$ [9]. Margaryan and Springer applied XEFT at LO to the decay $\psi(4160) \rightarrow X\gamma$ [10]. Recently, Jansen, Hammer and Jia used XEFT to determine the dependence of the binding energy of X on the light quark masses [11]. They also calculated the $D^{*0}\bar{D}^0$ scattering length to NLO and to leading order in m/M . The applications of XEFT are not limited to the $D\bar{D}\pi$ sector, which also includes $D^*\bar{D}$ and $D\bar{D}^*$ states. Canham, Hammer, and Springer pointed out that XEFT can be applied to the $DD\bar{D}\pi$ and $DD\bar{D}\pi\pi$ sectors [12]. They calculated the S-wave phase shifts for low-energy scattering of D or D^* from X at LO. Braaten, Hammer, and Mehen pointed out that XEFT can be applied to the $D\bar{D}\pi\pi$ sector, which also includes $D^*\bar{D}^*$, $D^*\bar{D}\pi$, and $D\bar{D}^*\pi$ states [13]. They calculated the low-energy cross sections for elastic π^+X scattering and for the break-up reaction $\pi^+X \rightarrow D^{*+}\bar{D}^0$ at LO.

We will refer to the formulation of XEFT presented in Ref. [6] as *original XEFT*. There are various problems with original XEFT that present obstacles to accurate quantitative predictions. Some of these problems are due to its formulation as a nonrelativistic field theory of the charm mesons and π^0 that is not Galilean invariant. One consequence of the lack of Galilean invariance is that a preferred frame (such as the center-of-momentum frame) must be specified either explicitly or implicitly in any calculation. Another consequence of the lack of Galilean invariance is that ultraviolet divergences are much less constrained. The explicit counterterms in the Lagrangian for original XEFT in Ref. [6] are sufficient to eliminate ultraviolet divergences in NLO calculations only if results are expanded in powers of m/M and then truncated at a sufficiently low order. This truncation provides a limit on the accuracy. Although the mass ratio $m/M = 0.072$ is very small, the expansion is actually in powers of the square root of the mass ratio, which is 0.27. The alternative of adding additional counterterms to the Lagrangian to cancel the ultraviolet divergences would introduce additional parameters that would have to be determined phenomenologically. Another problem with original XEFT is that the renormalization scheme made it difficult to take into account some decays into final states with momenta too large to be treated explicitly in XEFT. These decays are $D^{*0} \rightarrow D^0\gamma$, which accounts for about a third of the full width of the D^{*0} , and all decay modes of the $X(3872)$ other than $D^0\bar{D}^0\pi^0$.

Alhakami and Birse have recently proposed an alternative power counting for XEFT [14]. In their power counting, m and $M_* - M$ are treated as small energy scales of order Q , and δ is treated as a tiny energy scale of order Q^2/M . The ratios $\delta/m = 0.051$ and $m/M = 0.072$ are both of order Q/M . This power counting scheme was not implemented at the lagrangian level, but it provides an organizing principle for simplifying Feynman diagrams. The power counting of Ref. [14] makes the expansion in powers of m/M systematic. The formulation in Ref. [14] is convenient for matching onto heavy hadron chiral perturbation theory, which has been used in several applications of XEFT [7–10]. It does not address the problems of frame dependence or of additional ultraviolet divergences. With this new power counting, the decay D^{*0} into $D^0\gamma$ is within the domain of applicability of XEFT. However there are important decay modes of the $X(3872)$, such as $J/\psi\pi^+\pi^-$, that remain outside the domain of applicability of XEFT.

In this paper, we present a new formulation of XEFT that removes many of the obstacles to accurate quantitative calculations. The new formulation is an effective field theory with a Galilean symmetry that is motivated by the fact that mass is very nearly conserved in the transition $D^{*0} \rightarrow D^0\pi^0$. The Galilean symmetry solves the problem of frame dependence and it dramatically simplifies ultraviolet divergences. To take into account the decay $D^{*0} \rightarrow D^0\gamma$ and decay modes of the $X(3872)$ other than $D^0\bar{D}^0\pi^0$, a new renormalization scheme is introduced that is expressed

in terms of the complex energies of D^{*0} and $X(3872)$. The new Galilean-invariant formulation of XEFT is illustrated by a calculation of the $D^{*0}\bar{D}^0$ scattering length to NLO in the XEFT power counting. The cancellation of ultraviolet divergences for arbitrary values of m/M is verified explicitly.

II. GALILEAN-INVARIANT XEFT

In this section, we introduce a new formulation of XEFT as a Galilean-invariant field theory. We describe the changes in the Lagrangian for the original XEFT defined in Ref. [6] that are required for Galilean invariance. We explain how the effects of the decay $D^{*0} \rightarrow D^0\gamma$ can be taken into account through the complex rest energy of the D^{*0} . We then write down the next-to-leading order Lagrangian for Galilean-invariant XEFT, and give its Feynman rules.

A. Galilean Invariance

A unique feature of the decay $D^{*0} \rightarrow D^0\pi^0$ is that mass is very nearly conserved: the sum of the masses of the D^0 and π^0 is only about 3.5% lower than the mass of the D^{*0} . Galilean invariance is a possible space-time symmetry of a nonrelativistic theory that requires exact mass conservation [15]. The mass that must be conserved is the kinetic mass, which is the mass that appears in the denominator of the kinetic energy. The approximate conservation of mass in the transition $D^{*0} \rightarrow D^0\pi^0$ strongly motivates a Galilean-invariant formulation of XEFT. The Lagrangian for original XEFT, including all terms required to calculate the decay of $X(3872)$ into $D^0\bar{D}^0\pi^0$ to next-to-leading order (NLO), was written down in Ref. [6]. We will describe how the terms in this Lagrangian must be modified to make them Galilean invariant. The NLO Lagrangian for Galilean-invariant XEFT will be written down in Section II C.

We choose the kinetic masses of the D^0 and π^0 to be their physical masses M and m , respectively. Conservation of kinetic mass then requires the kinetic mass of D^{*0} to be $M + m$. The difference δ between the mass of the D^{*0} and its kinetic mass must be taken into account through its rest energy. Kinetic mass conservation requires the following change in the Lagrangian for original XEFT defined in Ref. [6]:

- In the kinetic term $\mathbf{D}^\dagger \cdot \nabla^2 \mathbf{D}/(2m_{D^*})$ for the D^{*0} , its mass m_{D^*} must be replaced by $M + m$.

A similar change must be made in the kinetic term for the \bar{D}^{*0} . It will be convenient to introduce the reduced kinetic mass μ for $D^{*0}\bar{D}^0$ and the reduced mass μ_π for $D^0\pi^0$:

$$\mu \equiv \frac{M(M+m)}{2M+m} = 965.0 \text{ MeV}, \quad (3a)$$

$$\mu_\pi \equiv \frac{mM}{M+m = 125.87 \text{ MeV}}. \quad (3b)$$

The ratio of these reduced masses is

$$r \equiv \frac{\mu_\pi}{\mu} = 0.1304. \quad (4)$$

Galilean invariance requires interaction terms to be invariant under Galilean boosts, in which the momenta of π^0 , D^0 , and D^{*0} are boosted by a common velocity vector \mathbf{v} multiplied by their kinetic masses m , M , and $M + m$, respectively. Galilean invariance requires three changes in the interaction terms in the Lagrangian for original XEFT that given in Ref. [6]:

- In the pion interaction term $\mathbf{D}^\dagger \cdot D \nabla \pi$, the operator ∇ between D and π should be replaced by $(M \vec{\nabla} - m \vec{\nabla})/(M + m)$.
- In the $\nabla^2 D^{*0}\bar{D}^0$ interaction term $(\bar{D}\mathbf{D})^\dagger \cdot \bar{D}(\vec{\nabla})^2 \mathbf{D}$, the operator $(\vec{\nabla})^2$ between \bar{D} and \mathbf{D} should be replaced by $4(M \vec{\nabla} - (M + m) \vec{\nabla})^2/(2M + m)^2$.
- In the interaction term $(\bar{D}\mathbf{D})^\dagger \cdot \bar{D}D \nabla \pi$ that describes the transition of $D^0\bar{D}^0\pi^0$ to $D^{*0}\bar{D}^0$, the operator ∇ between $\bar{D}D$ and π should be replaced by $(2M \vec{\nabla} - m \vec{\nabla})/(2M + m)$.

Similar changes must be made in the hermitian conjugates and charge conjugates of these interaction terms. The three modified interaction terms described above reduce to those of original XEFT in the limit $m/M \rightarrow 0$. The modified interaction terms ensure the invariance of amplitudes under Galilean boosts.

Galilean invariance also strongly constraints ultraviolet divergences. The changes above specify all terms in the Lagrangian for Galilean-invariant XEFT that are required to calculate the decay of $X(3872)$ into $D^0\bar{D}^0\pi^0$ to NLO in the XEFT power counting. The results should be independent of the ultraviolet cutoff to all orders in m/M . Without Galilean invariance, there are three independent $\nabla^2 D^{*0}\bar{D}^0$ interaction terms and two independent $D^0\bar{D}^0\pi^0 \rightarrow D^{*0}\bar{D}^0$ interaction terms. The Lagrangian for original XEFT defined in Ref. [6] includes only one interaction term of each kind. Cutoff independent results for the decay rate of $X(3872)$ into $D^0\bar{D}^0\pi^0$ at NLO were obtained by also truncating the expansion in powers of m/M at leading order.

Galilean-invariant XEFT can be extended to include charged charm mesons and charged pions. The π^+ must have the same kinetic mass m as π^0 . The D^+ must have the same kinetic mass M as D^0 . The D^{*+} must have the same kinetic mass $M + m$ as D^{*0} . The difference between the mass and kinetic mass of a particle must be taken into account through its rest energy.

In a nonrelativistic effective field theory for charm mesons, one can impose a phase symmetry that guarantees the separate conservation of the number N_c of charm quarks and the number $N_{\bar{c}}$ of charm antiquarks. These quark numbers can be expressed in terms of meson numbers:

$$N_c = N_{D^{*0}} + N_{D^0}, \quad (5a)$$

$$N_{\bar{c}} = N_{\bar{D}^{*0}} + N_{\bar{D}^0}. \quad (5b)$$

If one also considers charged charm mesons, the charm quark number N_c is the sum of the numbers of D^{*0} , D^{*+} , D^0 , and D^+ . In Galilean-invariant XEFT, the exact conservation of kinetic mass in the transitions $D^{*0} \leftrightarrow D^0\pi^0$ and $\bar{D}^{*0} \leftrightarrow \bar{D}^0\pi^0$ provides motivation for introducing an additional phase symmetry that guarantees the conservation of the *pion number* defined by

$$N_\pi = N_{\pi^0} + N_{D^{*0}} + N_{\bar{D}^{*0}}. \quad (6)$$

The name *pion number* is appropriate since the D^* can be interpreted as a P-wave $D\pi$ resonance. In Galilean-invariant XEFT with charged charm mesons and pions, the pion number is the sum of the numbers of π^0 , π^+ , π^- , D^{*0} , \bar{D}^{*0} , D^{*+} , and D^{*-} .

B. Choice of Rest Energies

In a nonrelativistic field theory, deviations from mass conservation in a reaction are taken into account through the rest energies of the particles involved. The rest energy of a particle can be chosen to be its physical mass. In a Galilean invariant theory, since the kinetic mass is conserved, the rest energy of a particle can equally well chosen as the difference between its physical mass and its kinetic mass. If there are linear combinations of the particle numbers that are conserved, field redefinitions can be used to set the rest energies of some of the particles to 0. In XEFT, conservation of the charm quark number N_c allows the rest energies of D^0 and D^{*0} to be set to 0 and $M_* - M$, respectively. Conservation of both N_c and the pion number N_π allows the rest energies of π^0 , D^0 , and D^{*0} to be set to 0, 0, and $\delta = M_* - M - m$, respectively.

The rest energy of a particle can also be used to take into account its partial width into decay modes that cannot be described explicitly in the effective field theory. Such a partial width is taken into account through a negative imaginary term in the rest energy. The width of D^{*0} is more than 5 orders of magnitude larger than the widths of D^0 and π^0 , so the widths of D^0 and π^0 can be completely ignored. The width of D^{*0} come from its decay into $D^0\pi^0$, which can be described explicitly in XEFT, and from its decay into $D^0\gamma$, whose momenta are too large to be described explicitly. The effect of the $D^0\gamma$ decay mode can be taken into account by including a term $-i\Gamma_{*,0,\gamma}/2$ in the D^{*0} rest energy, where $\Gamma_{*,0,\gamma}$ is the partial width of D^{*0} into $D^0\gamma$, whose branching fraction is approximately 38%. If we use the complex on-shell renormalization scheme for the D^{*0} propagator in which the position of the complex pole is specified, the D^{*0} rest energy also includes the term $-i\Gamma_{*,0,\pi}/2$, where $\Gamma_{*,0,\pi}$ is the partial width of D^{*0} into $D^0\pi^0$, whose branching fraction is approximately 62%. In this scheme, the complete imaginary part of the D^{*0} rest energy is $-i\Gamma_{*,0}/2$, where $\Gamma_{*,0} = \Gamma_{*,0,\pi} + \Gamma_{*,0,\gamma}$ is the full width of the D^{*0} .

In original XEFT, the rest energies of π^0 , D^0 , and D^{*0} were chosen to be $-\delta$, 0, and 0, respectively. Setting the rest energy of D^{*0} to 0 is inconvenient if we wish to take into account the partial width of D^{*0} into $D^0\gamma$. It is more convenient to choose the rest energies of π^0 and D^0 to be 0. The rest energy of D^{*0} is then $\delta - i\Gamma_{*,0}/2$. This requires the following change in the Lagrangian for original XEFT:

- The rest-energy term $\delta\pi^\dagger\pi$ for the π^0 should be replaced by the rest-energy term $-(\delta - i\Gamma_{*0}/2)\mathbf{D}^\dagger \cdot \mathbf{D}$ for the D^{*0} .

There is a similar rest-energy term for the \bar{D}^{*0} .

If Galilean-invariant XEFT is extended to include charged charm mesons and charged pions, mass differences and nonnegligible decay modes outside the domain of validity of the effective field theory can be taken into account through the rest energies of the particles. The $\pi^+ - \pi^0$ mass difference can be taken into account through the rest energy of π^+ . The $D^+ - D^0$ mass difference can be taken into account through the rest energy of D^+ . The difference between the $D^{*+} - D^0\pi^0$ mass difference can be taken into account through the rest energy of D^{*+} . The tiny partial width for the decay of D^{*+} into $D^+\gamma$ can also be taken into account through the rest energy of D^{*+} .

C. NLO Lagrangian

We can now write down the complete NLO Lagrangian for Galilean-invariant XEFT for the neutral charm mesons and the π^0 . It includes only those terms required to calculate the elastic scattering amplitude for $D^{*0}\bar{D}^0$ to NLO in the XEFT power counting. The field for the π^0 is denoted by π . The fields for the D^0 and \bar{D}^0 are denoted by D and \bar{D} . The fields for the D^{*0} and \bar{D}^{*0} are denoted by \mathbf{D} and $\bar{\mathbf{D}}$. The Lagrangian is the sum of kinetic terms, interaction terms, and counterterms.

There are kinetic terms for the π^0 , D^0 , \bar{D}^0 , and D^{*0} , and \bar{D}^{*0} . The kinetic terms for the π^0 , D^0 , and D^{*0} are

$$\mathcal{L}_{\pi^0} = \pi^\dagger (i\partial_0 + \nabla^2/(2m)) \pi, \quad (7a)$$

$$\mathcal{L}_{D^0} = D^\dagger (i\partial_0 + \nabla^2/(2M)) D, \quad (7b)$$

$$\mathcal{L}_{D^{*0}} = \mathbf{D}^\dagger \cdot (i\partial_0 + \nabla^2/(2(M+m))) \mathbf{D} - (\delta - i\Gamma_{*0}/2) \mathbf{D}^\dagger \cdot \mathbf{D}. \quad (7c)$$

The kinetic terms for the \bar{D}^0 and \bar{D}^{*0} can be obtained from those for D^0 and D^{*0} by replacing D by \bar{D} and \mathbf{D} by $\bar{\mathbf{D}}$.

The interaction terms consist of pion interactions, contact interactions, and ∇^2 interactions. The pion interaction terms for the transitions $D^{*0} \leftrightarrow D^0\pi^0$ are

$$\mathcal{L}_{D^{*0} \leftrightarrow D^0\pi^0} = \frac{g}{2\sqrt{m}f_\pi(M+m)} \left[\bar{\mathbf{D}}^\dagger \cdot (D[M\vec{\nabla} - m\vec{\nabla}] \pi) + (D[M\vec{\nabla} - m\vec{\nabla}] \pi)^\dagger \cdot \mathbf{D} \right]. \quad (8)$$

The pion interaction terms for the transitions $\bar{D}^{*0} \leftrightarrow \bar{D}^0\pi^0$ are obtained by replacing \mathbf{D} and D by $\bar{\mathbf{D}}$ and \bar{D} . The contact and ∇^2 interactions are the same in the $D^{*0}\bar{D}^0 \rightarrow D^{*0}\bar{D}^0$, $D^0\bar{D}^{*0} \leftrightarrow D^{*0}\bar{D}^0$, and $D^0\bar{D}^{*0} \rightarrow D^0\bar{D}^{*0}$ channels. The interaction terms in the $D^{*0}\bar{D}^0 \rightarrow D^{*0}\bar{D}^0$ channel are

$$\begin{aligned} \mathcal{L}_{D^{*0}\bar{D}^0 \rightarrow D^{*0}\bar{D}^0} = & -\frac{C_0}{2} (\bar{D}\mathbf{D})^\dagger \cdot (\bar{D}\mathbf{D}) \\ & + \frac{C_2}{4(2M+m)^2} \left[(\bar{D}\mathbf{D})^\dagger \cdot (\bar{D}[M\vec{\nabla} - (M+m)\vec{\nabla}]^2 \mathbf{D}) \right. \\ & \left. + (\bar{D}[M\vec{\nabla} - (M+m)\vec{\nabla}]^2 \mathbf{D})^\dagger \cdot (\bar{D}\mathbf{D}) \right]. \end{aligned} \quad (9)$$

The interaction terms in the other three channels are obtained by replacing \mathbf{D} and D by $\bar{\mathbf{D}}$ and \bar{D} in the appropriate places. The coupling constants g in Eq. (8) and C_0 and C_2 in Eq. (9) are essentially the same as those in the Lagrangian for original XEFT defined in Ref. [6].

To cancel ultraviolet divergences in Green functions at NLO, it is also necessary to include counterterms in the Lagrangian. The counterterms are the same in the $D^{*0}\bar{D}^0 \rightarrow D^{*0}\bar{D}^0$, $D^0\bar{D}^{*0} \leftrightarrow D^{*0}\bar{D}^0$, and $D^0\bar{D}^{*0} \rightarrow D^0\bar{D}^{*0}$ channels. The counterterms in the $D^{*0}\bar{D}^0 \rightarrow D^{*0}\bar{D}^0$ channel are

$$\mathcal{L}_{\text{counterterm}} = -\frac{\delta C_0}{2} (\bar{D}\mathbf{D})^\dagger \cdot (\bar{D}\mathbf{D}) - \frac{\delta D_0}{2} (\bar{D}\mathbf{D})^\dagger \cdot i\partial_t(\bar{D}\mathbf{D}). \quad (10)$$

The counterterm with coefficient δD_0 is not needed to calculate on-shell quantities, because it can be reduced to the other counterterm by using field redefinitions. It was omitted in Ref. [6], because the momentum distribution for $D^0\bar{D}^0\pi^0$ in the decay of the $X(3872)$ is an on-shell quantity.

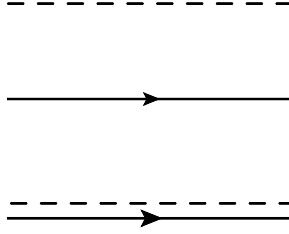


FIG. 1: The propagators for π^0 , D^0 , and D^{*0} are represented by dashed, solid, and solid+dashed lines, respectively. The Feynman rules for these propagators are given in Eqs. (11). The propagators for \bar{D}^0 and \bar{D}^{*0} look like those for D^0 and D^{*0} with the arrows reversed.

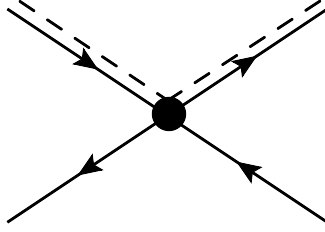


FIG. 2: The contact interaction vertex for $D^{*0}\bar{D}^0 \rightarrow D^{*0}\bar{D}^0$. The Feynman rule for this vertex is given in Eq. (13).

D. Feynman Rules

The terms in the NLO Lagrangian for Galilean-invariant XEFT with neutral charm mesons and the π^0 are given in Eqs. (7), (8), (9), and (10). We will give the Feynman rules for this Lagrangian. The Feynman rules that are actually used for calculations beyond leading order will be enclosed in boxes.

In XEFT, the charm quark and antiquark numbers N_c and $N_{\bar{c}}$ are conserved. In Galilean-invariant XEFT, the pion number N_π is also conserved. These conservation laws can all be made manifest in the Feynman rules by appropriate notation for the propagators. We use a dashed line for the pion propagator, a solid line for the D and \bar{D} propagators, and a double line consisting of a solid and a dashed line for the D^* and \bar{D}^* propagators. In the propagators for the mesons D^* and D that contain a charm quark, the solid line has a forward arrow. In the propagators for the mesons \bar{D}^* and \bar{D} that contain a charm antiquark, the solid line has a backward arrow. It is sometimes convenient to omit the arrows on internal lines of diagrams and to use the convention that there is an implied sum over the possible directions of the omitted arrows.

The propagators for the π^0 , D^0 , and D^{*0} are illustrated in Fig. 1. The Feynman rules for the propagators of the π^0 , the D^0 or \bar{D}^0 , and the D^{*0} or \bar{D}^{*0} are

$$\boxed{\frac{i}{p_0 - p^2/(2m) + i\epsilon}}, \quad (11a)$$

$$\boxed{\frac{i}{p_0 - p^2/(2M) + i\epsilon}}, \quad (11b)$$

$$\boxed{\frac{i\delta^{ij}}{p_0 - E_* - p^2/(2(M+m))}}, \quad (11c)$$

where p_0 and \mathbf{p} are the energy and momentum of the particle. The propagator of the D^{*0} is diagonal in its vector indices i and j , and its complex rest energy is

$$E_* = \delta - i\Gamma_{*0}/2. \quad (12)$$

Since E_* has a negative imaginary part, an explicit $i\epsilon$ prescription is unnecessary in the D^{*0} propagator.

At LO in the XEFT power counting, the only interaction that is required is a contact interaction for $D^{*0}\bar{D}^0$ in the $C = +$ channel. The Feynman rule for the vertex is the same for the $D^{*0}\bar{D}^0 \rightarrow D^{*0}\bar{D}^0$, $D^0\bar{D}^{*0} \leftrightarrow D^{*0}\bar{D}^0$, and $D^0\bar{D}^{*0} \rightarrow D^0\bar{D}^{*0}$ contact interactions:

$$(-iC_0/2)\delta^{ij}. \quad (13)$$

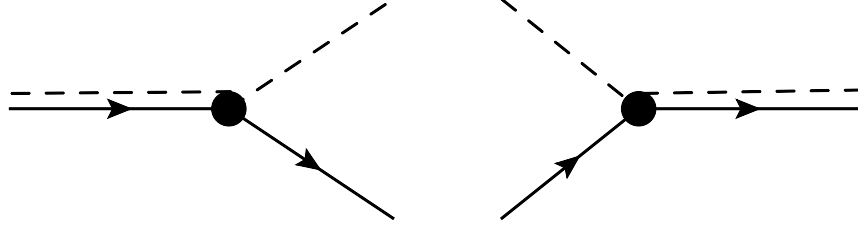


FIG. 3: The vertices for the pionic transitions $D^{*0} \rightarrow D^0\pi^0$ and $D^0\pi^0 \rightarrow D^{*0}$. The Feynman rule for the $D^{*0} \rightarrow D^0\pi^0$ vertex is given in Eq. (14).

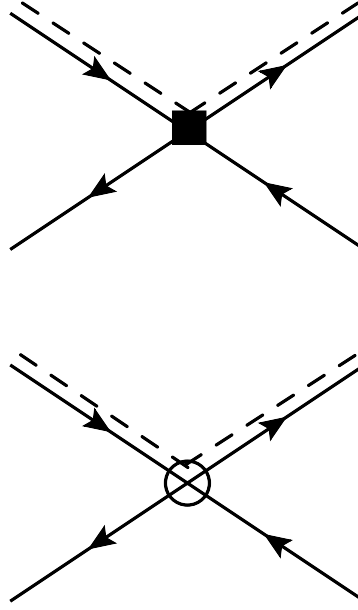


FIG. 4: The ∇^2 vertex and the counterterm vertex for $D^{*0}\bar{D}^0 \rightarrow D^{*0}\bar{D}^0$. The Feynman rules for these vertices are given in Eqs. (15) and (16), respectively.

This vertex for $D^{*0}\bar{D}^0 \rightarrow D^{*0}\bar{D}^0$ is illustrated in Fig. 2. The C_0 interaction must be treated nonperturbatively in XEFT. The set of subdiagrams consisting of an arbitrary number of successive C_0 interactions can be summed to all orders analytically. The Feynman rule for the resulting effective interaction is given later in Eq. (44). In calculations beyond leading order in XEFT, that effective vertex replaces the one in Eq. (13). That is why the Feynman rule in Eq. (13) is not enclosed in a box.

One of the interactions beyond LO in the XEFT power counting is the $D^* \leftrightarrow D\pi$ transition. The Feynman rules for the $D^{*0} \rightarrow D^0\pi^0$ and $\bar{D}^{*0} \rightarrow \bar{D}^0\pi^0$ vertices in Galilean-invariant XEFT are

$$\boxed{\frac{g}{2\sqrt{m}f_\pi} \frac{(M\mathbf{q} - m\mathbf{p})^i}{M + m}}, \quad (14)$$

where \mathbf{q} and \mathbf{p} are the momenta of the outgoing π^0 and charm meson, respectively. The vertices for $D^{*0} \rightarrow D^0\pi^0$ and $D^0\pi^0 \rightarrow D^{*0}$ are illustrated in Fig. 3. In the $D^0\pi^0$ center-of-momentum frame defined by $\mathbf{p} + \mathbf{q} = 0$, the momentum-dependent factor in Eq. (14) reduces to q^i , which is the momentum-dependent factor in all frames in original XEFT. The Feynman rules for the $D^0\pi^0 \rightarrow D^{*0}$ and $\bar{D}^0\pi^0 \rightarrow \bar{D}^{*0}$ vertices differ from Eq. (14) by an overall minus sign if \mathbf{q} and \mathbf{p} are the momenta of the incoming π^0 and charm meson, respectively. A convenient way to implement the XEFT power counting is to assign orders in g to the coupling constants of all other interaction terms. A complete calculation then requires calculating all diagrams to a given order in g .

The other interaction at NLO in the XEFT power counting is the ∇^2 interaction for $D^{*0}\bar{D}^0$ in the $C = +$ channel. The Feynman rule for the vertex is the same for the $D^{*0}\bar{D}^0 \rightarrow D^{*0}\bar{D}^0$, $D^0\bar{D}^{*0} \leftrightarrow D^{*0}\bar{D}^0$, and $D^0\bar{D}^{*0} \rightarrow D^0\bar{D}^{*0}$

interactions. In Galilean-invariant XEFT, the Feynman rule is

$$\boxed{(-iC_2/4) \frac{((M+m)\mathbf{p} - M\mathbf{p}_*)^2 + ((M+m)\mathbf{p}' - M\mathbf{p}'_*)^2}{(2M+m)^2} \delta^{ij}}, \quad (15)$$

where \mathbf{p} and \mathbf{p}_* are the momenta of the incoming spin-0 and spin-1 charm mesons and \mathbf{p}' and \mathbf{p}'_* are the momenta of the outgoing mesons. The vertex for $D^{*0}\bar{D}^0 \rightarrow D^{*0}\bar{D}^0$ is illustrated in Fig. 4. In the $D^{*0}\bar{D}^0$ center-of-momentum frame defined by $\mathbf{p}_* + \mathbf{p} = \mathbf{p}'_* + \mathbf{p}' = 0$, the momentum-dependent factor in Eq. (15) reduces to $p^2 + p'^2$. In this frame, the Feynman rule coincides with that in original XEFT, for which the momentum-dependent factor is $[(\mathbf{p} - \mathbf{p}_*)^2 + (\mathbf{p}' - \mathbf{p}'_*)^2]/4$. The coupling constant C_2 in Eq. (15) can be assigned order g^2 .

In addition to these interaction vertices, it is also necessary to include a counterterm vertex for $D^{*0}\bar{D}^0$ in the $C = +$ channel. The vertex is the same for the $D^{*0}\bar{D}^0 \rightarrow D^{*0}\bar{D}^0$, $D^0\bar{D}^{*0} \leftrightarrow D^{*0}\bar{D}^0$, and $D^0\bar{D}^{*0} \rightarrow D^0\bar{D}^{*0}$ interactions:

$$\boxed{(-i[\delta C_0 + \delta D_0 E]/2) \delta^{ij}}, \quad (16)$$

where E is the total energy of the pair of charm mesons. The counterterm vertex for $D^{*0}\bar{D}^0 \rightarrow D^{*0}\bar{D}^0$ is illustrated in Fig. 4. The δD_0 term is not needed to calculate on-shell quantities at NLO, but it is needed to cancel ultraviolet divergences in off-shell Green functions. The counterterm coefficients δC_0 and δD_0 in Eq. (16) can be assigned order g^2 .

In the original paper on XEFT, an additional interaction term that produces a transition of $D^{*0}\bar{D}^0$ to $D^0\bar{D}^0\pi^0$ was written down explicitly [6]. The Feynman rule for its vertex in Galilean-invariant XEFT is

$$\boxed{\frac{B_1}{2\sqrt{m}} \frac{(2M\mathbf{q} - m(\mathbf{p} + \bar{\mathbf{p}}))^i}{2M + m}}, \quad (17)$$

where \mathbf{q} , \mathbf{p} , and $\bar{\mathbf{p}}$ are the outgoing momenta of the pion and the two spin-0 charm mesons. In the $D^0\bar{D}^0\pi^0$ center-of-momentum frame defined by $\mathbf{p} + \bar{\mathbf{p}} + \mathbf{q} = 0$, the momentum-dependent factor in Eq. (17) reduces to q^i , which is the momentum-dependent factor in all frames in original XEFT. The coupling constant B_1 in Eq. (17) can be assigned order g^3 . This interaction term was needed in Ref. [6] to calculate the decay of $X(3872)$ into $D^0\bar{D}^0\pi^0$ to NLO in the XEFT power counting or, equivalently, to relative order g^2 .

In the D^{*0} propagator in Eq. (11c), a wavefunction renormalization factor Z can be inserted in the numerator. That factor can be made completely arbitrary by inserting canceling factors of $Z^{-1/2}$ into the interaction vertices for each D^{*0} or \bar{D}^{*0} line. The number of such factors in the interaction vertices in Eqs. (13), (14), (15), and (16) would be 2, 1, 2, and 2, respectively. These factors can be absorbed into the coupling constants.

If we use dimensional regularization with d spatial dimensions, it is useful to introduce a renormalization scale Λ to keep the dimensions of coupling constants the same as in the physical dimension $d = 3$. The interaction vertices in Eqs. (13), (14), (15), and (16) would be multiplied by Λ raised to the powers $3-d$, $(3-d)/2$, $3-d$, and $3-d$, respectively. In a Green function, the net effect of these powers of Λ is a factor of Λ^{3-d} for every loop integral and an overall multiplicative factor of Λ^{3-d} raised to some power. The factor of Λ^{3-d} associated with a loop integral can be absorbed into its integration measure. If the Green function is made finite by renormalization, the overall multiplicative factor of Λ^{3-d} raised to some power can be simply be ignored, because it is equal to 1 in the physical dimension $d = 3$.

III. RENORMALIZATION PRESCRIPTIONS

In this section, we introduce renormalization prescriptions that can be used to take into account the effects of transitions to states in which the momenta are too large to be described explicitly in XEFT. We also calculate the transition amplitude for $D^{*0}\bar{D}^0 \rightarrow D^{*0}\bar{D}^0$ at leading order in XEFT.

A. $D^* - D\pi$ Coupling Constant

One of the coupling constants in XEFT beyond leading order is the $D^* - D\pi$ coupling constant $g/\sqrt{2}f_\pi$. It could in principle be determined from the partial width of D^{*0} into $D^0\pi^0$:

$$\Gamma_{*,0,\pi} \equiv \Gamma[D^{*0} \rightarrow D^0\pi^0] = \left(\frac{g^2}{4mf_\pi^2} \right) \frac{\mu_\pi}{3\pi} (2\mu_\pi\delta)^{3/2}, \quad (18)$$

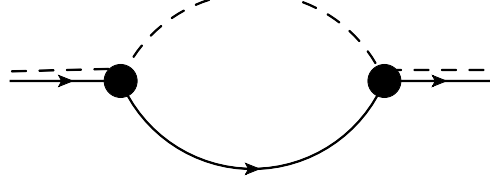


FIG. 5: The one-loop (and only) D^{*0} self-energy diagram in XEFT. The diagram with external legs amputated can be expressed as $-i\Sigma(E_{\text{cm}})\delta^{ij}$.

where δ is the mass difference in Eq. (2) and μ_π is the $D\pi$ reduced mass defined in Eq. (3b). The branching fraction for $D^{*0} \rightarrow D^0\pi^0$ has been measured to be $(62 \pm 3)\%$, but the full width of D^{*0} has not been measured.

By exploiting isospin symmetry, the coupling constant $g/\sqrt{2}f_\pi$ can also be determined from decays of the D^{*+} . The full width of D^{*+} has been recently measured with high precision by the Babar Collaboration [17]: $\Gamma[D^{*+}] = 83.3 \pm 1.2 \pm 1.4$ keV. The sum of the branching fractions of D^{*+} into $D^0\pi^+$ and $D^+\pi^0$ is 0.984 ± 0.005 . In Galilean-invariant XEFT, the sum of the partial widths into $D^0\pi^+$ and $D^+\pi^0$ is

$$\Gamma[D^{*+} \rightarrow D^0\pi^+] + \Gamma[D^{*+} \rightarrow D^+\pi^0] = \frac{1}{3\pi} \left(\frac{g^2}{4mf_\pi^2} \right) \mu_\pi \left[2(2\mu_\pi\delta_{+0})^{3/2} + (2\mu_\pi\delta_{++})^{3/2} \right], \quad (19)$$

where $\delta_{+0} = 5.856 \pm 0.002$ MeV is the $D^{*+} - D^0\pi^+$ mass difference, and $\delta_{++} = 5.68 \pm 0.08$ MeV is the $D^{*+} - D^+\pi^0$ mass difference. The resulting value of the coupling constant g is given by

$$\frac{g^2}{4mf_\pi^2} = (3.67 \pm 0.08) \times 10^{-8} \text{ MeV}^{-3}. \quad (20)$$

The pion decay constant f_π determines the scattering amplitude for $\pi\pi$ scattering. With the convention for f_π used in Ref. [6], its value is $f_\pi \approx 132$ MeV. Given that value, the pion transition coupling constant in Eq. (20) is determined to be $g \approx 0.59$. A more appropriate dimensionless measure of the strength of the pion exchange interaction in XEFT is

$$\frac{g^2\mu^2\sqrt{2\mu_\pi\delta}}{12\pi mf_\pi^2} \approx 0.15, \quad (21)$$

where μ is the reduced kinetic mass of $D^{*0}\bar{D}^0$ defined in Eq. (3a).

The determination of the values of g and f_π separately is unnecessary in XEFT applied to the $D\bar{D}\pi$ sector (which includes $D^*\bar{D}$), because the number of pions in the system can only be 0 or 1. In the $D\bar{D}\pi\pi$ sector (which includes $D^*\bar{D}^*$), the number of pions in the system can be 0, 1, or 2. Since there can be contributions from $\pi\pi$ scattering, the value of f_π is needed at a sufficiently high order in the XEFT power counting.

B. D^{*0} Propagator

The conservation of pion number in Galilean-invariant XEFT implies that the exact D^{*0} propagator can be calculated analytically. It can be obtained by summing a geometric series of the one-loop D^{*0} self-energy diagram in Figure 5. Galilean invariance implies that the propagator for a D^{*0} with energy p_0 and momentum \mathbf{p} is a function of the Galilean-invariant combination

$$E_{\text{cm}} = p_0 - \frac{\mathbf{p}^2}{2(M+m)}. \quad (22)$$

The exact D^{*0} propagator can be expressed as

$$D_*^{ij}(p_0, \mathbf{p}) = \frac{i[1 + \delta Z]\delta^{ij}}{E_{\text{cm}} - (E_* + \delta E_*) - \Sigma(E_{\text{cm}})}, \quad (23)$$

where $\Sigma(E_{\text{cm}})$ is the D^{*0} self-energy and δE_* is a rest-energy counterterm. We have introduced a wavefunction renormalization factor $1 + \delta Z$ in the numerator. It can be made completely arbitrary by absorbing canceling factors

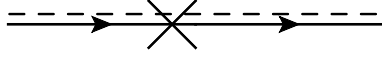


FIG. 6: The D^{*0} self-energy counterterm vertex. The Feynman rule for this vertex at order g^2 in the complex on-shell scheme is given in Eq. (31).

of $[1 + \delta Z]^{-1/2}$ into the interaction vertices. With dimensional regularization, the D^{*0} self-energy is

$$\Sigma(E_{\text{cm}}) = -\mu_\pi \left(\frac{g^2}{4m f_\pi^2} \right) \frac{\Lambda^{3-d}\Gamma(-d/2)}{(4\pi)^{d/2}} [e^{-i\pi} 2\mu_\pi E_{\text{cm}}]^{d/2}, \quad (24)$$

where Λ is the renormalization scale and μ_π is the $D^0\pi^0$ reduced mass in Eq. (3b). The self-energy has cubic and linear ultraviolet divergences that are manifested as single poles in d and $d - 2$, respectively. The pole in $d - 2$ is

$$\frac{1}{d-2} \lim_{d \rightarrow 2} (d-2)\Sigma(E_{\text{cm}}) = \left(\frac{g^2}{4m f_\pi^2} \right) \frac{2\mu_\pi^2 \Lambda}{3\pi(d-2)} E_{\text{cm}}. \quad (25)$$

In the physical dimension $d = 3$, the self-energy is pure imaginary for real positive E_{cm} :

$$\lim_{d \rightarrow 3} \Sigma(E_{\text{cm}}) = -i \left(\frac{g^2}{4m f_\pi^2} \right) \frac{\mu_\pi}{6\pi} [2\mu_\pi E_{\text{cm}}]^{3/2}. \quad (26)$$

Its value at $E = \delta$ is $-i\Gamma_{*0,\pi}/2$, where $\Gamma_{*0,\pi}$ is the partial width of D^{*0} into $D^0\pi^0$ given in Eq. (18).

In the *minimal power-divergence subtraction* (PDS) renormalization scheme [16], the D^{*0} rest energy and the propagator counterterms are

$$E_{*,\text{PDS}} = \delta, \quad (27a)$$

$$\delta E_{*,\text{PDS}} = 0, \quad (27b)$$

$$\delta Z_{\text{PDS}} = - \left(\frac{g^2}{4m f_\pi^2} \right) \frac{2\mu_\pi^2 \Lambda}{3\pi(d-2)}. \quad (27c)$$

In the physical dimension $d = 3$, the self-energy $\Sigma(E_{\text{cm}})$ reduces to Eq. (26). The approximate position of the pole in p_0 of the D^{*0} propagator in Eq. (23) is where E_{cm} is equal to the complex energy $\delta - i\Gamma_{*0,\pi}/2$. The PDS scheme does not take into account the decay $D^{*0} \rightarrow D^0\gamma$.

The pole in the energy p_0 for the physical D^{*0} propagator occurs when E_{cm} is equal to the complex energy $E_* = \delta - i\Gamma_{*0}/2$, where Γ_{*0} is the full width of the D^{*0} . We introduce the *complex on-shell* (COS) renormalization scheme for the D^{*0} propagator in which its pole in p_0 is at the complex physical value and the residue of that pole is the same as at LO. The D^{*0} rest energy and the propagator counterterms are

$$E_* = \delta - i\Gamma_{*0}/2, \quad (28a)$$

$$\delta E_* = -\Sigma(E_*), \quad (28b)$$

$$\delta Z = -\Sigma'(E_*), \quad (28c)$$

where $\Sigma(E)$ is the self-energy in Eq. (24). In the physical dimension $d = 3$, δE_* and δZ in the COS scheme reduce to

$$\lim_{d \rightarrow 3} \delta E_* = -i \left(\frac{g^2}{4m f_\pi^2} \right) \frac{\mu_\pi}{6\pi} [2\mu_\pi E_*]^{3/2}, \quad (29a)$$

$$\lim_{d \rightarrow 3} \delta Z = i \left(\frac{g^2}{4m f_\pi^2} \right) \frac{\mu_\pi^2}{2\pi} [2\mu_\pi E_*]^{1/2}. \quad (29b)$$

If we ignore the tiny difference between $E_* = \delta - i\Gamma_{*0}/2$ and δ , the rest energy counterterm in Eq. (29a) reduces to $\delta E_* = -i\Gamma_{*0,\pi}/2$, where $\Gamma_{*0,\pi}$ is the partial width of the D^{*0} into $D^0\pi^0$ in Eq. (18).

Although Eq. (23) is the exact D^{*0} propagator in Galilean-invariant XEFT, it is not practical to use this propagator in loop diagrams, because the term in the denominator proportional to $E_{\text{cm}}^{d/2}$ makes loop integrals more complicated to evaluate. It is better to expand the exact propagator in Eq. (23) in powers of g^2 :

$$D_*^{ij}(p_0, p) = \frac{i\delta^{ij}}{E_{\text{cm}} - E_*} \sum_{N=0}^{\infty} \left[\frac{\Sigma(E_{\text{cm}}) + \delta E_* + \delta Z(E_{\text{cm}} - E_*)}{[1 + \delta Z](E_{\text{cm}} - E_*)} \right]^N. \quad (30)$$

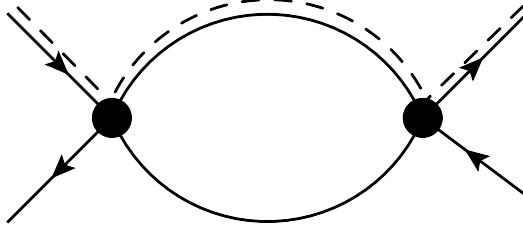


FIG. 7: The one-loop diagram for the LO $D^{*0}\bar{D}^0$ transition amplitude. There is an implied sum over the two possible directions of the arrows on the internal lines. The diagram with external legs amputated can be expressed as the contact interaction vertex $(-iC_0/2)\delta^{ij}$ multiplied by $C_0\Pi(E_{\text{cm}})$, where $\Pi(E_{\text{cm}})$ is the LO $D^{*0}\bar{D}^0$ self-energy.

The expansion generates a geometric series of propagator corrections. The terms of order g^2 correspond to inserting into the propagator the one-loop D^{*0} self-energy subdiagram in Fig. 6 and a D^{*0} self-energy counterterm. The Feynman rule for the order- g^2 self-energy counterterm vertex in the COS scheme is

$$\boxed{+i\left(\Sigma(E_*) + \Sigma'(E_*)[p_0 - p^2/(2(M+m)) - E_*]\right)\delta^{ij}}, \quad (31)$$

where p_0 and p are the energy and momentum of the D^{*0} , i and j are its vector indices, and $\Sigma(E)$ is the self-energy in Eq. (24).

The previous NLO calculations in XEFT were carried out in the original version of XEFT, which is not Galilean invariant. The D^{*0} self-energy $\Sigma(p_0, p)$ is therefore a function of the two independent variables p_0 and p . The kinetic mass of the D^{*0} was set equal to its physical mass M_* . The D^{*0} rest energy was taken to be the real energy δ , although it was actually taken into account through the rest energy term for the π^0 . In the NLO calculation of the decay of $X(3872)$ into $D^0\bar{D}^0\pi^0$ in Ref. [6], the renormalization of the D^{*0} propagator was carried out using the minimal power divergence subtraction scheme in Eq. (27). In the physical dimension $d = 3$, the counterterm δZ_{PDS} in Eq. (27c) reduces to the renormalization scale Λ multiplied by a constant. This term was cancelled by a kinetic counterterm for the D^{*0} .

In the NLO calculation of the $D^{*0}\bar{D}^0$ scattering length In Ref. [11], the complex energy of the $X(3872)$ and its partial width into $D^0\bar{D}^0\pi^0$ were calculated to NLO using original XEFT. The calculation involved a two-loop diagram that has a one-loop D^{*0} self-energy subdiagram and that diverges as $1/p$ as the relative momentum p of $D^{*0}\bar{D}^0$ approaches 0. The divergence was avoided by resumming to all orders terms proportional to $\Gamma_{*0,\pi}^{1/2}$ from one-loop D^{*0} self-energy subdiagrams. The resummation could have been implemented in such a way that the terms that were resummed had only integer powers of $\Gamma_{*0,\pi}$. This is equivalent to the complex on-shell renormalization scheme for the D^{*0} propagator in Eq. (28), but with E_* replaced by $\delta - i\Gamma_{*0,\pi}/2$. The imaginary part of E_* is not equal to the physical value $-\Gamma_{*0}/2$, because the decay $D^{*0} \rightarrow D^0\gamma$ was not taken into account in Ref. [11].

C. $D^{*0}\bar{D}^0$ Transition Amplitude

In XEFT, the conservation of pion number ensures that loop diagrams in the $D\bar{D}\pi$ sector have a single D or \bar{D} propagator in every loop. The integral over the loop energy of a D can therefore be evaluated by closing the contour around the pole in the D propagator, putting the D on its energy shell. Since D or \bar{D} lines in loops can be put on their energy shells, it is sufficient to consider Green functions in which all external D or \bar{D} lines are on their energy shells.

The amputated connected Green function for $D^{*0}\bar{D}^0 \rightarrow D^{*0}\bar{D}^0$ in the $C = +$ channel, with the incoming and outgoing \bar{D}^0 or D^0 on their energy shells, can be expressed as $+i\mathcal{A}^{ij}$, where the tensor \mathcal{A}^{ij} is a function of the total energy P_0 and the momenta of the two incoming and two outgoing particles. Its vector indices are associated with the polarizations of the incoming and outgoing D^{*0} or \bar{D}^{*0} . In XEFT, the corresponding amplitude in the $C = -$ channel is 0. We will refer to \mathcal{A}^{ij} as the transition amplitude for $D^{*0}\bar{D}^0$ in the $C = +$ channel or simply as the *transition amplitude*. Its contribution to the amplitude for $D^{*0}\bar{D}^0 \rightarrow D^{*0}\bar{D}^0$ is $+i\mathcal{A}^{ij}/2$, where the factor of $(1/\sqrt{2})^2$ comes from projections onto the $C = +$ channel.

The tree level term in the LO transition amplitude, which is given by the Feynman rule in Eq. (13), is $-C_0\delta^{ij}$. The $D^{*0}\bar{D}^0$ coupling constant C_0 must be treated nonperturbatively in order to generate the bound state that can be identified with the $X(3872)$. The one-loop diagram in Fig. 7 is therefore also LO. The complete LO transition

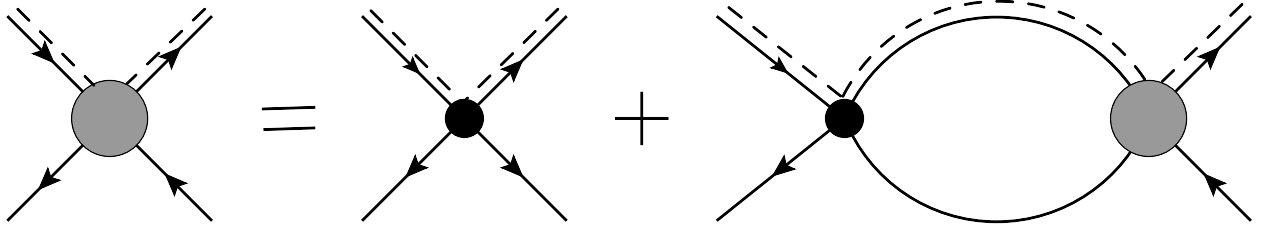


FIG. 8: The Lippmann-Schwinger integral equation for the LO $D^{*0}\bar{D}^0$ transition amplitude. In the second diagram on the right side, there is an implied sum over the two possible directions of the arrows on the internal lines. The Feynman rule for the LO transition amplitude is given in Eq. (44).

amplitude can be obtained by summing a geometric series of the one-loop diagrams. This sum is equivalent to the solution of the Lippmann-Schwinger equation shown in Figure 8.

In Galilean-invariant XEFT, the LO transition amplitude depends on the energies and momenta of the initial-state and final-state particles only through the Galilean-invariant combination

$$E_{\text{cm}} = P_0 - \frac{\mathbf{P}^2}{2(2M+m)}, \quad (32)$$

where P_0 is the total energy of the D^{*0} and \bar{D}^0 relative to the $D^0\bar{D}^0\pi^0$ threshold and \mathbf{P} is their total momentum. The LO transition amplitude is $(2\pi/\mu)\mathcal{A}(E_{\text{cm}})\delta^{ij}$, where

$$\mathcal{A}(E_{\text{cm}}) = \frac{\mu/(2\pi)}{-[C_0^{-1} + \delta C_0^{-1}] + \Pi(E_{\text{cm}})} \quad (33)$$

and $\Pi(E_{\text{cm}})$ is a function of E_{cm} that we will refer to as the $D^{*0}\bar{D}^0$ *self-energy*. The inverse coupling constant from the contact interaction vertex in Eq. (13) has been separated into C_0^{-1} and a LO counterterm δC_0^{-1} . Despite the notation, δC_0^{-1} is independent of the NLO counterterm δC_0 in the counterterm vertex in Eq. (16). With dimensional regularization, the $D^{*0}\bar{D}^0$ self-energy is

$$\Pi(E_{\text{cm}}) = -2\mu \frac{\Lambda^{3-d}\Gamma(1-d/2)}{(4\pi)^{d/2}} [2\mu(E_* - E_{\text{cm}})]^{d/2-1}, \quad (34)$$

where μ is the reduced kinetic mass of $D^{*0}\bar{D}^0$ defined in Eq. (3a). If the amplitude $\mathcal{A}(E_{\text{cm}})$ in Eq. (33) has a pole in P_0 , the residue of the pole is

$$Z_X = -\frac{(4\pi)^{d/2-1}\Lambda^{d-3}}{2\mu\Gamma(2-d/2)} \gamma_X^{4-d}. \quad (35)$$

This is a smooth function of d for $d < 4$.

The $D^{*0}\bar{D}^0$ self-energy has a linear ultraviolet divergence that is manifested by a pole in $d-2$:

$$\frac{1}{d-2} \lim_{d \rightarrow 2} (d-2)\Pi(E_{\text{cm}}) = \frac{\mu\Lambda}{\pi(d-2)}. \quad (36)$$

In the minimal power-divergence subtraction (PDS) scheme [16], this pole is cancelled by a LO counterterm:

$$(\delta C_0^{-1})_{\text{PDS}} = \frac{\mu\Lambda}{\pi(d-2)}. \quad (37)$$

The LO transition amplitude in Eq. (33) then has a finite limit as $d \rightarrow 2$:

$$\lim_{d \rightarrow 2} \mathcal{A}(E_{\text{cm}}) = \frac{1}{\log(2\mu(E_* - E_{\text{cm}})/\Lambda_2^2)\Lambda}. \quad (38)$$

The momentum scale Λ_2 in the logarithm is determined by the limiting behavior of C_0^{-1} as $d \rightarrow 2$.

In the physical dimension $d = 3$, the LO transition amplitude in Eq. (33) reduces to the form

$$\lim_{d \rightarrow 3} \mathcal{A}(E_{\text{cm}}) = \frac{1}{-\gamma_X + \sqrt{-2\mu(E_{\text{cm}} - E_*)}}, \quad (39)$$

where γ_X is a complex constant that we will refer to as the *binding momentum* of the $X(3872)$. It is determined by the limiting behavior of C_0^{-1} as $d \rightarrow 3$:

$$\gamma_X = (2\pi/\mu) \lim_{d \rightarrow 3} (C_0^{-1} + \delta C_0^{-1}). \quad (40)$$

The amplitude $\mathcal{A}(E_{\text{cm}})$ in Eq. (33) has a pole in P_0 on the physical sheet. The residue of the pole is

$$\lim_{d \rightarrow 3} Z_X = -\gamma_X/\mu. \quad (41)$$

The pole in P_0 of the amplitude $\mathcal{A}(E_{\text{cm}})$ in Eq. (33) occurs when E_{cm} equals a complex energy E_X that can be interpreted as the energy of the $X(3872)$ resonance:

$$E_X = E_* - \gamma_X^2/(2\mu) \quad (42a)$$

$$= \delta - \delta_X - i\Gamma_X/2. \quad (42b)$$

In the first line, the complex energy E_X has been expressed in terms of the complex D^{*0} energy E_* and the complex binding momentum γ_X . In the second line, E_X has been expressed in terms of real variables δ_X and Γ_X that can be interpreted as the binding energy and full width of the $X(3872)$. The measured value of the binding energy δ_X is given in Eq. (1). The width Γ_X has not yet been measured, but there is an upper bound: $\Gamma_X < 1.2$ MeV [18]. If the complex binding momentum is expressed as $\gamma_X = \gamma_{\text{re}} + i\gamma_{\text{im}}$, where γ_{re} and γ_{im} are real, the binding energy and full width are

$$\delta_X = (\gamma_{\text{re}}^2 - \gamma_{\text{im}}^2)/(2\mu), \quad (43a)$$

$$\Gamma_X = \Gamma_{*0} + 2\gamma_{\text{re}}\gamma_{\text{im}}/\mu. \quad (43b)$$

In calculations beyond LO in the XEFT power counting, it is convenient to replace the contact interaction vertex in Eq. (13) by a vertex for the transition amplitude. The Feynman rules are the same for the $D^{*0}\bar{D}^0 \rightarrow D^{*0}\bar{D}^0$, $D^0\bar{D}^{*0} \leftrightarrow D^{*0}\bar{D}^0$, and $D^0\bar{D}^{*0} \rightarrow D^0\bar{D}^{*0}$ transition amplitudes:

$$+i\left(\frac{1}{\sqrt{2}}\right)^2 \frac{2\pi}{\mu} \mathcal{A}(E_{\text{cm}}) \delta^{ij},$$

(44)

where E_{cm} is the function of the total energy P_0 and the total momentum P of the charm meson pair defined in Eq. (32) and i and j are the vector indices of the incoming and outgoing D^{*0} . In d dimensions, the function $\mathcal{A}(E_{\text{cm}})$ is defined by Eqs. (33) and (34). In the physical dimension $d = 3$, it reduces to Eq. (39). The vertex for the transition amplitude is represented by a blob, as illustrated for the $D^{*0}\bar{D}^0 \rightarrow D^{*0}\bar{D}^0$ channel by the Lippmann-Schwinger equation in Fig. 8.

Beyond leading order in the XEFT power counting, the transition amplitude $\mathcal{A}^{ij}(E_{\text{cm}}, \mathbf{p}, \mathbf{p}')$ for $D^{*0}\bar{D}^0$ in the $C = +$ channel in Galilean invariant XEFT is a function of E_{cm} and the relative momenta \mathbf{p} and \mathbf{p}' of the incoming and outgoing charm mesons. At NLO, this amplitude has additional ultraviolet divergences. The renormalizability of XEFT requires that they be cancelled by appropriate choices of the constants δC_0 and δD_0 in the counterterm vertex in Eq. (16). A renormalization prescription for the amplitude $\mathcal{A}^{ij}(E_{\text{cm}}, \mathbf{p}, \mathbf{p}')$ is necessary to determine the finite parts after the cancellations. In order to take into account decay modes of the $X(3872)$ with momenta too large to be described explicitly, it is advantageous to use the *complex on-shell* (COS) renormalization scheme in which the pole in the total energy P_0 is at its physical value. The complex energy of the pole can be specified in terms of the complex binding momentum γ_X of the $X(3872)$, as in Eq. (42a), or in terms of its binding energy δ_X and full width Γ_X , as in Eq. (42b). The definition of the COS scheme for the $D^{*0}\bar{D}^0 \rightarrow D^{*0}\bar{D}^0$ Green function can be completed by specifying the residue of the pole in P_0 . The amplitude $\mathcal{A}^{ij}(E_{\text{cm}}, \mathbf{p}, \mathbf{p}')$ has a well-behaved limit as $\mathbf{p} \rightarrow 0$ and $\mathbf{p}' \rightarrow 0$ that is a function of E_{cm} only. Thus we complete the definition of the COS scheme by requiring the residue of the pole in P_0 for the amplitude $\mathcal{A}^{ij}(E_{\text{cm}}, 0, 0)$ to be the same as for the LO amplitude $(2\pi/\mu)\mathcal{A}(E_{\text{cm}})\delta^{ij}$. In the physical dimension $d = 3$, the limiting behavior as P_0 approaches the pole is

$$\mathcal{A}^{ij}(E_{\text{cm}}, 0, 0) \longrightarrow \frac{(2\pi/\mu)Z_X\delta^{ij}}{[P_0 - P^2/(2(2M+m))] - [E_* - \gamma_X^2/(2\mu)]}, \quad (45)$$

where Z_X is the LO residue in Eq. (41) and γ_X is the complex binding momentum of the $X(3872)$. The COS scheme can be implemented through specific choices of the counterterms δC_0 and δD_0 .

In the previous NLO calculations in XEFT in Ref. [6] and [11], the NLO counterterm δC_0 was included, but δD_0 was not. The counterterm δC_0 could have been chosen so that the pole in P_0 was at the physical point, as in Eq. (45). However without the counterterm δD_0 , the prescription in Eq. (45) for the residue of the pole could not have been implemented. In fact, the residue would have been ultraviolet divergent.

IV. $D^{*0}\bar{D}^0$ SCATTERING

In this Section, we use Galilean-invariant XEFT to calculate the $D^{*0}\bar{D}^0$ scattering length to NLO in the XEFT power counting.

A. NLO Transition Amplitude

In Galilean-invariant XEFT, the NLO transition amplitude for $D^{*0}\bar{D}^0 \rightarrow D^{*0}\bar{D}^0$ in the $C = +$ channel in the center-of-momentum frame is a tensor $\mathcal{A}^{ij}(E, \mathbf{p}, \mathbf{p}')$ that depends on the total energy E and the relative momenta \mathbf{p} and \mathbf{p}' of the incoming and outgoing charm mesons. The LO transition amplitude is $(2\pi/\mu)\mathcal{A}(E)\delta^{ij}$, where $\mathcal{A}(E)$ in the physical dimension $d = 3$ is given in Eq. (39). The NLO diagrams for the transition amplitude are calculated in Appendix B. The 20 diagrams are labeled A_n , B_n , C_n , and D_n , where n is an integer. The NLO terms in the transition amplitude have a well-behaved limit as $\mathbf{p} \rightarrow 0$ and $\mathbf{p}' \rightarrow 0$ that is diagonal in the vector indices i and j . The NLO transition amplitude can be expressed as

$$\begin{aligned} \mathcal{A}^{ij}(E, 0, 0) = & \frac{2\pi}{\mu} \left(\mathcal{A}(E) + (g^2\mu^2/4mf_\pi^2)[F(E)\mathcal{A}^2(E) + G(E)\mathcal{A}(E)] \right. \\ & \left. + (C_2/C_0)H(E)\mathcal{A}^2(E) - \frac{2\pi[\delta C_0 + \delta D_0 E]}{\mu C_0^2}\mathcal{A}^2(E) \right) \delta^{ij}. \end{aligned} \quad (46)$$

The NLO correction terms either have a factor of $\mathcal{A}^2(E)$ or a factor of $\mathcal{A}(E)$. The function $F(E)$, which has dimensions of momentum, is obtained by adding the pion-exchange diagram $A4$ in Eq. (B8) and the D^* propagator correction diagrams $B1$ and $B2$ in Eqs. (B9) and (B10). The function $H(E)$, which is dimensionless, is the sum of the pion-exchange diagrams $A2$ and $A3$ in Eq. (B7). The function $G(E)$, which has dimensions of (momentum) 3 , comes from the ∇^2 vertex diagrams C in Eqs. (B16). The δC_0 and δD_0 terms come from the $D^*\bar{D}$ counterterm diagrams D in Eq. (B18). The functions $F(E)$, $G(E)$, and $H(E)$ can be expressed in terms of the loop integrals J_n , I_n , and K_{lmn} defined in Appendix A:

$$\begin{aligned} F(E) = & \frac{(-8\pi)r}{d} \left(\frac{1}{\sqrt{1-r}} [2K_{110}(E) - 2\mu(2E_* - rE)K_{111}(E) - (2-r)J_1(E)^2] \right. \\ & \left. + 2[K_{110}(E) - 2\mu E_* K_{120}(E)] + rI_1(E_*)[4\mu E_* J_2(E) - dJ_1(E)] \right), \end{aligned} \quad (47a)$$

$$G(E) = \frac{8r\sqrt{1-r}[(E - E_*)J_1(E) - rEI_1(E)]}{d[(1-r)E - E_*]}, \quad (47b)$$

$$H(E) = 8\pi\mu(E - E_*)J_1(E), \quad (47c)$$

where $r = \mu_\pi/\mu$ is the ratio of reduced masses defined in Eq. (4). The terms proportional to $\mathcal{A}(E)$ in Eq. (46) have a single pole in E at $E_* - \gamma_X^2/(2\mu)$. The terms proportional to $\mathcal{A}^2(E)$ have an unphysical double pole in E . The N²LO term would have a triple pole and higher order terms would have even higher poles. These unphysical multiple poles can be summed to all orders, in which case they produce a shift in the position of the pole in the LO amplitude. In Ref. [11], such a resummation was used in the NLO calculations of the binding energy of the $X(3872)$ and its partial width into $D^0\bar{D}^0\pi^0$. It was not used in the NLO calculation of the $D^{*0}\bar{D}^0$ scattering length. An expression for the transition amplitude that is accurate to NLO and has only a single pole is

$$\mathcal{A}^{ij}(E, 0, 0) = \frac{(2\pi/\mu)[1 + (g^2\mu^2/4mf_\pi^2)G(E)]\delta^{ij}}{\mathcal{A}(E)^{-1} - (g^2\mu^2/4mf_\pi^2)F(E) - (C_2/C_0)H(E) + (2\pi/\mu C_0^2)[\delta C_0 + \delta D_0 E]}. \quad (48)$$

To NLO accuracy, the factor of $1 + (g^2\mu^2/4mf_\pi^2)G$ in the numerator could equally well be moved to the denominator as a factor $1 - (g^2\mu^2/4mf_\pi^2)G$ multiplying $\mathcal{A}(E)^{-1}$.

B. Renormalization

Loop integrals in XEFT have ultraviolet (UV) divergences. With dimensional regularization, the UV divergences produce poles in $d - 2$ and poles in $d - 3$. A pole in $d - 3$ represents a logarithmic UV divergence, and a pole in $d - 2$ represents a linear UV divergence. In previous NLO calculations in XEFT [6, 11], power divergence subtraction

was used to remove the poles in $d - 2$. The subsequent limit $d \rightarrow 3$ produces terms that depend explicitly on the renormalization scale Λ . In the PDS scheme, a loop integral with a pole term $\Lambda^{3-d}/(d-2)$ requires a canceling counterterm $-\Lambda/(d-2)$. In the physical dimension $d = 3$, the loop integral becomes independent of Λ , but the canceling counterterm reduces to $-\Lambda$.

In the NLO calculation of the decay of the $X(3872)$ into $D^0\bar{D}^0\pi^0$ in Ref. [6], the explicit dependence on Λ was through terms proportional to Λ , Λ^2 , and $\log \Lambda$. The explicit dependence on Λ was exactly cancelled by the implicit dependence on Λ of the coupling constants of XEFT. In the NLO calculations of Ref. [11], in addition to terms proportional to Λ , Λ^2 , $\log \Lambda$, there was explicit dependence on Λ from terms proportional to $1/(\Lambda - \gamma)$, where γ is the leading order binding momentum or inverse scattering length. These terms were introduced by a resummation prescription for dealing with an infrared divergence at the $D^{*0}\bar{D}^0$ threshold. The terms proportional to $1/(\Lambda - \gamma)$ were not cancelled by the implicit dependence on Λ of the coupling constants, but they were suppressed by a factor proportional to the partial width $\Gamma_{*,0,\pi}$ for $D^{*0} \rightarrow D^0\pi^0$.

The poles in $d - 3$ in the NLO transition amplitude are given in Appendix B in Eqs. (B22). In the NLO transition amplitude in Eq. (46), the only poles in $d - 3$ come from the two-loop integrals K_{110} , K_{120} , and K_{111} in the function $F(E)$ in Eq. (47a). The poles in K_{120} and K_{111} are constants given in Eqs. (A20b) and (A20c), respectively. The pole in K_{110} is a linear function of E given in Eq. (A23). Thus the dependence on the energy in the pole terms is of the form $\mathcal{A}^2(E)$ and $E\mathcal{A}^2(E)$. These poles in $d - 3$ can be cancelled by the δC_0 and δD_0 counterterms in Eq. (46). Thus logarithmic UV divergences in the NLO transition amplitude can be cancelled by the available counterterms.

The poles in $d - 2$ in the NLO transition amplitude are given in Appendix B in Eqs. (B20) and (B21). In the NLO transition amplitude in Eq. (46), the functions $G(E)$ and $H(E)$ have single poles in $d - 2$ while the function $F(E)$ has double poles. The single poles in $d - 2$ in the one-loop integrals J_1 and I_1 are given in Eqs. (A14). The poles in $d - 2$ in the two-loop integrals are given in Eqs. (A18): K_{110} has a double pole and K_{120} has a single pole. The pole terms with the energy dependence $\mathcal{A}^2(E)$ and $E\mathcal{A}^2(E)$ can be cancelled by the counterterms δC_0 and δD_0 , respectively. They include the double-pole terms from $F(E)$, some of the single-pole terms from $F(E)$, and the single-pole terms from $H(E)$. However there are also single-pole terms from $F(E)$ that have the energy dependence $\log(E_* - E)\mathcal{A}(E)^2$. In the single pole of $G(E)$ in Eq. (47b), the energy-dependent denominator is cancelled, so it gives pole terms with the energy dependence $\mathcal{A}(E)$. Neither of these terms can be cancelled by the available counterterms δC_0 and δD_0 . The poles in $d - 2$ after suitable choices of the counterterms are

$$\begin{aligned} \mathcal{A}^{ij}(E) &\rightarrow \left(\frac{g^2}{4mf_\pi^2} \right) \frac{4r\sqrt{1-r}\mu\Lambda^2}{d-2} \log \frac{2\mu(E_* - E)}{\Lambda^2} \mathcal{A}^2(E) \delta^{ij} \\ &+ \left(\frac{g^2}{4mf_\pi^2} \right) \frac{(-4)r\sqrt{1-r}\mu\Lambda}{d-2} \mathcal{A}(E) \delta^{ij}. \end{aligned} \quad (49)$$

The argument of the logarithm has been made dimensionless by using the renormalization scale Λ .

The uncanceled poles in $d - 2$ in Eq. (49) seem to indicate that the NLO transition amplitude in Galilean-invariant XEFT has linear UV divergences that cannot be removed by renormalization. This puzzle can be resolved by taking into account the expression for the amplitude $\mathcal{A}(E)$ in $d = 2$, which is given in Eq. (38). Its reciprocal $\mathcal{A}(E)^{-1}$ is linear in $\log(E_* - E)$. The cancellation between the two terms in Eq. (49) leaves a term with the energy dependence $\mathcal{A}^2(E)$ that can be cancelled by the counterterm δC_0 .

We proceed to implement the complex on-shell renormalization scheme specified by Eq. (45). This scheme requires the pole in E of $\mathcal{A}^{ij}(E, 0, 0)$ to be at the same complex energy E_X and to have the same residue as the LO amplitude $(2\pi/\mu)\mathcal{A}(E)\delta^{ij}$. It can be implemented as specific choices of the counterterms δC_0 and δD_0 . We use the variation of the amplitude in Eq. (48) in which the term $(g^2\mu^2/4mf_\pi^2)G$ in the numerator is moved to the denominator. The renormalized expression for the transition amplitude is

$$\begin{aligned} \mathcal{A}^{ij}(E, 0, 0) &= (2\pi/\mu)\delta^{ij} [\mathcal{A}(E)^{-1} - (g^2\mu^2/4mf_\pi^2)[G(E)\mathcal{A}(E)^{-1} - G(E_X)(E - E_X)/Z_X] \\ &\quad - (g^2\mu^2/4mf_\pi^2)F_{\text{sub}}(E) - (C_2/C_0)H_{\text{sub}}(E)]^{-1}, \end{aligned} \quad (50)$$

where $F_{\text{sub}}(E)$ and $H_{\text{sub}}(E)$ are obtained by subtracting terms from $F(E)$ and $H(E)$:

$$F_{\text{sub}}(E) = F(E) - F(E_X) - F'(E_X)(E - E_X), \quad (51a)$$

$$H_{\text{sub}}(E) = H(E) - H(E_X) - H'(E_X)(E - E_X). \quad (51b)$$

The denominator in Eq. (50) vanishes at $E = E_X$. The value of its first derivative at $E = E_X$ is such that the residue of the pole in E is $(2\pi/\mu)Z_X\delta^{ij}$, in accord with the renormalization prescription in Eq. (45). The explicit expressions

for the counterterms are given by

$$\begin{aligned} \frac{2\pi\delta C_0}{\mu C_0^2} &= \frac{g^2\mu^2}{4mf_\pi^2} \left(F(E_X) - [F'(E_X) + G(E_X)/Z_X]E_X \right) \\ &\quad + \frac{C_2}{C_0} \left(H(E_X) - H'(E_X)E_X \right), \end{aligned} \quad (52a)$$

$$\frac{2\pi\delta D_0}{\mu C_0^2} = \frac{g^2\mu^2}{4mf_\pi^2} [F'(E_X) + G(E_X)/Z_X] + \frac{C_2}{C_0} H'(E_X). \quad (52b)$$

In the previous NLO calculations in XEFT in Refs. [6] and [11], power divergence subtraction was used to make double and single poles in $d - 2$ explicit as terms proportional to Λ^2 and Λ , where Λ is the renormalization scale. Since the poles in $d - 2$ have the same energy dependence as the counterterms δC_0 and δD_0 , the terms proportional to Λ^2 and Λ are exactly cancelled by those counterterms in the COS scheme. Thus it is unnecessary to use power divergence subtraction to make the poles in $d - 2$ explicit.

C. $D^{*0}\bar{D}^0$ Scattering Length

T-matrix elements in XEFT involving charm mesons and π^0 's can be obtained from the amputated connected Green functions by the following steps:

- Multiply by a polarization vector ε^i for a D^{*0} or \bar{D}^{*0} in the initial state and by a polarization vector ε'^j* for a D^{*0} in the final state.
- Multiply by a residue factor $|Z_*|^{1/2}$ for each D^{*0} or \bar{D}^{*0} in the initial and final states. In the COS scheme, $Z_* = 1$.
- Put the external lines on their energy shells. For the D^0 or \bar{D}^0 and for the π^0 , the energy shells are real: $p_0 = p^2/(2M)$ and $p_0 = p^2/(2m)$, respectively. For the D^{*0} or \bar{D}^{*0} , the energy shell is complex: $p_0 = E_* + p^2/(2(M+m))$.

We consider the elastic scattering of $D^{*0}\bar{D}^0$ in the center-of-momentum frame with incoming momenta $\pm p\hat{\mathbf{z}}$ and outgoing momenta $\pm p\hat{\mathbf{n}}$. The scattering angle satisfies $\cos\theta = \hat{\mathbf{z}} \cdot \hat{\mathbf{n}}$. The initial and final polarization vectors of the D^{*0} are ε and ε' . The total energy is $E_p = E_* + p^2/(2\mu)$. The T-matrix element is

$$\mathcal{T}(p, \theta) = (1/2) \sum_{ij} \mathcal{A}^{ij}(E_p, p\hat{\mathbf{z}}, p\hat{\mathbf{n}}) \varepsilon^i \varepsilon'^j*. \quad (53)$$

In the limit of zero relative momentum, the scattering is isotropic. The T-matrix element reduces to

$$\mathcal{T}(p=0) = (1/2) \sum_{ij} \mathcal{A}^{ij}(E_*, 0, 0) \varepsilon^i \varepsilon'^j*, \quad (54)$$

where the transition amplitude is given by Eq. (50) evaluated at $E = E_*$.

In the case of short-range interactions, a scattering amplitude can be expanded in powers of the relative momentum. This expansion is called the *effective range expansion*. Beyond LO in XEFT, the effective range expansion for $D^{*0}\bar{D}^0$ breaks down because of the effects of the exchange of a pion that can be on its energy shell. However Jansen, Hammer, and Jia pointed out that the leading term in the effective range expansion, which is the S-wave $D^{*0}\bar{D}^0$ scattering length, remains well defined [11]. They calculated the scattering length to NLO in original XEFT, truncating the expression at first order in an expansion in powers of $\gamma_X/\sqrt{2m\delta}$ and at leading order in m/M . We will calculate the scattering length to NLO in Galilean-invariant XEFT, truncating the expression at fourth order in an expansion in powers of $\gamma_X/\sqrt{2\mu E_*}$ but keeping all orders in m/M .

The S-wave scattering length $a_{s,+}$ for $D^{*0}\bar{D}^0$ in the $C = +$ channel can be defined by expressing the T-matrix in the zero-momentum limit in Eq. (54) as

$$\mathcal{T}(p=0) = (1/2)(2\pi/\mu)(-a_{s,+})\varepsilon \cdot \varepsilon'^*. \quad (55)$$

At leading order in XEFT, the inverse scattering length is equal to the complex binding momentum: $1/a_{s,+} = \gamma_X$. The inverse scattering length at NLO is

$$\begin{aligned} 1/a_{s,+} &= \gamma_X + (g^2\mu^2/4mf_\pi^2)[G(E_X) - 2G(E_*)]\gamma_X/2 \\ &\quad + (g^2\mu^2/4mf_\pi^2)F_{\text{sub}}(E_*) + (C_2/C_0)H_{\text{sub}}(E_*). \end{aligned} \quad (56)$$

We have used the expressions for E_X and Z_X in terms of γ_X in Eqs. (42a) and (41). This expression for $1/a_{s,+}$ in Eq. (56) can be simplified by expanding it in powers of $\gamma_X/\sqrt{2\mu E_*}$ using the expressions for the one-loop integrals J_n and I_n in Eqs. (A21a) and (A22a) and the threshold expansions for the two-loop integrals K_{lmn} in Eqs. (A30). The expansion of $G(E_X) - 2G(E_*)$ to third order in γ_X is

$$G(E_X) - 2G(E_*) \approx -\frac{2i}{3\pi} r^{3/2} \sqrt{1-r} \sqrt{2\mu E_*} \left(1 + \frac{(2+r)\gamma_X^2}{2r(2\mu E_*)} - \frac{i\gamma_X^3}{r^{3/2}(2\mu E_*)^{3/2}} \right), \quad (57)$$

where $r = \mu_\pi/\mu$ is the ratio of reduced masses defined in Eq. (4). The quantity $H_{\text{sub}}(E_*)$ is very simple:

$$H_{\text{sub}}(E_*) = \gamma_X^3/2. \quad (58)$$

The expansion of $F_{\text{sub}}(E_*)$ to fourth order in γ_X is

$$\begin{aligned} F_{\text{sub}}(E_*) \approx & -i \frac{r^{5/2}[1-\sqrt{1-r}]}{6\pi\sqrt{1-r}} \gamma_X \sqrt{2\mu E_*} \\ & + \frac{1}{12\pi^2} \left(-\frac{r^{5/2}}{5} + \frac{(12-22r-5r^2)r^{1/2}}{3\sqrt{1-r}} + \frac{(2-r)(2-4r-r^2)\arccos(\sqrt{r})}{1-r} \right. \\ & \left. + \frac{8(2-r)}{\sqrt{1-r}} {}_2F_1\left(-\frac{1}{2}, -\frac{1}{2}, \frac{3}{2}, 1-r\right) \right) \frac{\gamma_X^4}{2\mu E_*}. \end{aligned} \quad (59)$$

Our final result for the inverse scattering length, including all terms suppressed by up to three powers of $\gamma_X/\sqrt{2\mu E_*}$, is

$$\begin{aligned} 1/a_{s,+} = & \gamma_X + \frac{C_2}{2C_0} \gamma_X^3 + \frac{g^2 \mu^2}{12\pi m f_\pi^2} \left[-ir^{3/2} \left(1 - \frac{1}{2}r + \frac{1}{8}r^2 \right) \gamma_X \sqrt{2\mu E_*} \right. \\ & - ir^{1/2} \left(1 - \frac{3}{8}r^2 \right) \frac{\gamma_X^3}{\sqrt{2\mu E_*}} \\ & \left. + \left(1 - \frac{1}{2}r - \frac{1}{8}r^2 - \frac{1}{10\pi}r^{5/2} \right) \frac{\gamma_X^4}{2\mu E_*} \right]. \end{aligned} \quad (60)$$

The coefficient of each term has been expanded to relative order $r^{5/2}$. The leading power of r in the $g^2\gamma_X$ term comes from the function G . The entire $g^2\gamma_X^3$ term comes from the function G . The $g^2\gamma_X^4$ term receives contributions of order r^0 from both the function F and the function G .

D. Comparison with Previous Calculation

We can compare our result for the scattering length $a_{s,+}$ in Eq. (60) with that from a previous calculation by Jansen, Hammer, and Jia [11]. They used original XEFT to calculate the complex energy E_X of the $X(3872)$ and the complex scattering length $a_{s,+}$, dropping terms that were suppressed by at least one power of $r = m/M$. They expressed their results in terms of a leading-order inverse scattering length γ . Their physical renormalization condition was that the real part of the complex energy E_X should be identified with the energy of the $X(3872)$ resonance. Their NLO corrections included terms proportional to g^2 , C_2 , and an additional coupling constant D_2 that takes into account the dependence of the contact interaction on the pion mass. The coupling constant D_2 allowed them to study the dependence of the mass of the $X(3872)$ on the light quark masses. Their NLO corrections also included terms involving the partial width $\Gamma_{*0,\pi}$ for $D^{*0} \rightarrow D^0\pi^0$ that were resummed to all orders. If the other NLO corrections are omitted, their results reduce to

$$E_X = \delta - \gamma^2/(2\mu) - i\Gamma_{*0,\pi}/2, \quad (61a)$$

$$a_{s,+} = 1/\left(\gamma - \sqrt{-i\mu\Gamma_{*0,\pi}}\right), \quad (61b)$$

where $\Gamma_{*0,\pi}$ is the partial width of D^{*0} into $D^0\pi^0$. The universal relation expressing the binding energy in terms of a large positive scattering length $a_{s,+}$ is

$$E_X = \delta - 1/(2\mu a_{s,+}^2). \quad (62)$$

The leading order results in Eqs. (61) are incompatible with the analytic continuation of this universal relation to a complex scattering length $a_{s,+}$. This incompatibility suggests that the resummation used in Ref. [11] to eliminate an infrared divergence at the $D^{*0}\bar{D}^0$ threshold was inadequate. Because of this problem, we will only compare results in the limit $\Gamma_{*0,\pi} \rightarrow 0$. In this limit, their NLO results reduce to

$$E_X = \delta - \frac{\gamma^2}{2\mu} \left(1 + \frac{(C_2/C_0)(4\pi\gamma/\mu) + (g^2\mu/6\pi f_\pi^2)(1/\gamma)[(\Lambda - \gamma)^2 - 2m\delta d'_2]}{1 + (g^2\mu/6\pi f_\pi^2)(m\delta/\gamma)\log(1 + 2i\gamma/\sqrt{2m\delta})} \right), \quad (63a)$$

$$a_{s,+} = \frac{1}{\gamma} - \frac{1}{\gamma^2} \left(\frac{g^2\mu}{12\pi f_\pi^2} \right) \left[-2i\gamma\sqrt{2m\delta} + \Lambda^2 - 2\gamma\Lambda - 2m\delta d'_2 \right], \quad (63b)$$

where Λ is the PDS renormalization scale and d'_2 is a finite constant related to the coupling constant D_2 . Note that the dependence on Λ can be eliminated from both E_X and from $a_{s,+}$ by absorbing it into d'_2 . In the expression for $a_{s,+}$ in Eq. (63b), the factor of $1/\gamma^2$ comes from a term that has an unphysical double pole in the energy. The double pole could have been eliminated in favor of a shift in the position of the single pole by expressing $a_{s,+}$ as the ratio of a numerator and denominator with NLO accuracy, as in their result for E_X in Eq. (63a).

The complex on-shell renormalization scheme can be implemented by choosing d'_2 so that the numerator of the NLO correction term to E_X in Eq. (63a) is zero. The complex energy E_X then reduces to $\delta - \gamma^2/(2\mu)$, so γ can be identified with the binding momentum γ_X of the $X(3872)$. The NLO scattering length calculated in Ref. [11] reduces to

$$a_{s,+} = \frac{1}{\gamma_X} \left[1 + \frac{2\pi C_2}{\mu C_0^2} \gamma_X + \frac{g^2\mu}{12\pi f_\pi^2} \left(2i\sqrt{2m\delta} - \gamma_X \right) \right]. \quad (64)$$

This can be compared with the result from Galilean-invariant XEFT in Eq. (60). Dropping terms suppressed by three or more powers of $\gamma_X/\sqrt{2\mu E_*}$ and keeping only the leading power of r in the coefficients, our result reduces to

$$a_{s,+} = \frac{1}{\gamma_X} \left[1 - \frac{C_2}{2C_0} \gamma_X^2 + \frac{g^2\mu^2}{12\pi m f_\pi^2} \left(ir^{3/2} \sqrt{2\mu E_*} + ir^{1/2} \frac{\gamma_X^2}{\sqrt{2\mu E_*}} \right) \right]. \quad (65)$$

If we ignore the tiny difference between E_* and δ and if we approximate μ by $M/2$ and μ_π by m , the $\sqrt{2\mu E_*}$ term in Eq. (65) agrees with the $\sqrt{2m\delta}$ term in Eq. (64). However the other correction terms in Eq. (64) are proportional to γ_X , while those in Eq. (65) are proportional to γ_X^2 . Furthermore the coupling constants C_2 and C_0 appear in the combination C_2/C_0^2 in Eq. (64), while they appear in the combination C_2/C_0^2 in Eq. (65). Thus there seems to be a clear discrepancy between the results for $a_{s,+}$ in Eqs. (64) and (65). However the conclusion that there is a discrepancy relies on an implicit assumption that the coupling constant C_2 in Eqs. (64) and (65) can be identified. In the following section, we will show the surprising result that in the limit $g \rightarrow 0$ in which the pions decouple, the NLO correction terms proportional to C_2 in Eqs. (64) and (65) are indeed compatible. Whether the apparent discrepancy between the NLO correction terms proportional to $g^2\gamma_X$ in Eq. (64) and to $g^2\gamma_X^2$ in Eq. (65) is real cannot be determined definitively using the results given in Ref. [11].

E. Decoupled Pions

If pions are decoupled by setting $g = 0$, the NLO terms in the transition amplitude $\mathcal{A}^{ij}(E, \mathbf{p}, \mathbf{p}')$ reduces to the ∇^2 vertex diagrams C in Eqs. (B16) and the $D^*\bar{D}$ counterterm diagrams D in Eq. (B18). The terms proportional to $\mathcal{A}^2(E)$ which have a double pole in E , can to NLO accuracy be replaced by terms in the denominator, as in Eq. (48). After implementing the COS renormalization scheme, the transition amplitude reduces to

$$\mathcal{A}^{ij}(E, p, p') = \frac{(2\pi/\mu)[1 + \frac{1}{2}(C_2/C_0)(p^2 + p'^2)]}{\mathcal{A}(E)^{-1} - (C_2/C_0)H_{\text{sub}}(E)} \delta^{ij}, \quad (66)$$

where $H_{\text{sub}}(E)$ is defined by Eqs. (51b) and (47c).

To obtain the T-matrix element in Eq. (53), we put the charm mesons on their energy shells by setting $p' = p$ and setting the energy equal to $E_p = E_* + p^2/(2\mu)$. The term $H_{\text{sub}}(E_p)$ in the denominator of Eq. (66) is

$$H_{\text{sub}}(E_p) = \frac{1}{2}\gamma_X^3 + \frac{3}{2}\gamma_X p^2 + ip^3. \quad (67)$$

The T-matrix element reduces to

$$\mathcal{T}(p) = \frac{(\pi/\mu)[1 + (C_2/C_0)p^2]}{-\gamma_X - ip - (C_2/C_0)[\frac{1}{2}\gamma_X^3 + \frac{3}{2}\gamma_X p^2 + ip^3]} \epsilon \cdot \epsilon'^*. \quad (68)$$

To NLO accuracy, the factor $1 + (C_2/C_0)p^2$ in the numerator of Eq. (68) could equally be included as a factor $1 - (C_2/C_0)p^2$ multiplying $-\gamma_X - ip$ in the denominator:

$$\mathcal{T}(p) = \frac{\pi/\mu}{-[\gamma_X + \frac{1}{2}(C_2/C_0)\gamma_X^3] - \frac{1}{2}(C_2/C_0)\gamma_X p^2 - ip} \epsilon \cdot \epsilon'^*. \quad (69)$$

We can read off the S-wave inverse scattering length and effective range in the $C = +$ channel as coefficients in the denominator:

$$1/a_{s,+} = \gamma_X + \frac{1}{2}(C_2/C_0)\gamma_X^3, \quad (70a)$$

$$r_{s,+} = -(C_2/C_0)\gamma_X. \quad (70b)$$

The inverse scattering length in Eq. (70a) is consistent to NLO accuracy with setting $g = 0$ in Eq. (60). Eliminating C_2/C_0 , we reproduce a familiar relation between the scattering length, effective range, and binding momentum to first order in the range expansion:

$$1/a_{s,+} = \gamma_X \left(1 - \frac{1}{2}r_{s,+}\gamma_X\right). \quad (71)$$

Our result for the effective range in Eq. (70b) implies that, in the absence of pions, the ratio C_2/C_0 of coupling constants has a simple physical interpretation in terms of the effective range and the binding momentum:

$$C_2/C_0 = -r_{s,+}/\gamma_X. \quad (72)$$

In the previous NLO calculations in XEFT in Refs. [6] and [11], power divergence subtraction was used and C_0 and C_2 were determined as functions of the renormalization scale Λ . The dependence on Λ canceled in the following combination of coupling constants:

$$C_2/C_0^2 = \mu r_{s,+}/(4\pi). \quad (73)$$

The apparent incompatible with our result in Eq. (72) is at first puzzling. Our coupling constants C_0 and C_2 can be defined as the coefficients of the terms in the Lagrangian given in Eq. (9). This seems to be equivalent to the definitions of C_0 and C_2 in Ref. [6] up to corrections suppressed by powers of $r = \mu_\pi/M_\pi$. The resolution is that the absence of the counterterm δD_0 in the Lagrangian for original XEFT in Ref. [6] implies that the definitions are not equivalent. To determine the relation between the coupling constants, it is necessary to compare physical observables, such as the effective range $r_{s,+}$. By equating $r_{s,+}$ in Eqs. (72) and (73), we can infer that the combination C_2/C_0^2 in Ref. [6] should actually be identified with our ratio C_2/C_0 multiplied by $-\mu\gamma_X/(4\pi)$. This identification brings the NLO correction terms to $a_{s,+}$ proportional to $(C_2/C_0^2)\gamma_X$ in Eq. (64) and $(C_2/C_0)\gamma_X^2$ in Eq. (65) into agreement.

V. SUMMARY

We have introduced a Galilean-invariant formulation of XEFT to exploit the fact that mass is very nearly conserved in the transition $D^* \rightarrow D\pi$. Galilean invariance requires the kinetic mass of the D^* to be equal to the sum of the kinetic masses M and m of the D and π . One advantage of Galilean invariance is that an amplitude is the same in every Galilean frame. A more important advantage is that it strongly constrains the form of ultraviolet divergences. The operators in the NLO Lagrangian for Galilean-invariant XEFT can be obtained by making minor modifications in the terms of the NLO Lagrangian for original XEFT. NLO calculations in Galilean-invariant XEFT are ultraviolet finite for arbitrary values of the masses M and m . In contrast, NLO calculations in original XEFT are ultraviolet finite only if they are expanded in powers of m/M and truncated at a sufficiently low order.

We also introduced the complex on-shell (COS) renormalization prescription that takes into account the effects of transitions to states that cannot be described explicitly in XEFT. These transitions include the decay $D^{*0} \rightarrow D^0\pi^0$, which accounts for about 38% of the total width of the D^{*0} . They also include the decays of $X(3872)$ to all final states other than $D^0\bar{D}^0\pi^0$. These other decay modes may account for a substantial fraction of the total width of the $X(3872)$. The COS prescription requires as input the total width of the D^{*0} and the total width of the $X(3872)$, which has not yet been measured.

We illustrated the use of Galilean-invariant XEFT by calculating the transition amplitude for $D^{*0}\bar{D}^0 \rightarrow D^{*0}\bar{D}^0$ to NLO in the XEFT power counting. We used dimensional regularization in d spatial dimensions to regularize the ultraviolet divergences. The NLO Lagrangian includes counterterms that can cancel terms whose energy dependence has the form $\mathcal{A}^2(E)$ and $E\mathcal{A}^2(E)$, where $\mathcal{A}(E)$ is the LO transition amplitude. It was straightforward to verify that the logarithmic ultraviolet divergences, which appeared as poles in $d - 3$, could be cancelled by the counterterms.

The cancellation of linear ultraviolet divergences, which appeared as poles in $d - 2$, was not as straightforward. In addition to the poles that could be cancelled by the counterterms, there were additional poles in $d - 2$ whose energy dependence had the form $\mathcal{A}^2(E) \log(E_* - E)$ and $\mathcal{A}(E)$. They cancelled each other only upon using the specific form of the LO transition amplitude $\mathcal{A}(E)$ for $d = 2$.

We used our NLO result for the transition amplitude to calculate the $D^{*0}\bar{D}^0$ scattering length $a_{s,+}$ to NLO. Our result differs in several respects from a previous result for $a_{s,+}$ calculated using original XEFT in Ref. [11]. One important difference is in the effect of the D^{*0} width. Our COS renormalization prescription ensures that the effect of the D^{*0} width is in accord with the universal relation between the binding energy of an S-wave bound state near threshold and the scattering length of its constituents. The effect of the partial width of the D^{*0} into $D^0\pi^0$ in Ref. [11] is incompatible with the universal relation. This suggests that the resummation used in Ref. [11] to deal with an infrared divergence at the $D^{*0}\bar{D}^0$ threshold was inadequate. There is an apparent disagreement between our result and that of Ref. [11] in the NLO corrections to $a_{s,+}$ proportional to C_2 , but we showed that the difference is actually due to different definitions of C_2 . Our NLO correction to $a_{s,+}$ proportional to g^2 was expanded in powers of $\gamma_X/\sqrt{2m\delta}$, where γ_X is the binding momentum of the $X(3872)$. The leading term is proportional to $g^2\sqrt{2m\delta}$, and it agrees with that in Ref. [11] in the limit $m/M \rightarrow 0$. The next term in our expansion is second order in γ_X , while there is a term in Ref. [11] that is first order in γ_X . The origin of this discrepancy has not been determined.

Our Galilean-invariant formulation of XEFT removes obstacles to precise calculations of the properties of the $X(3872)$ resonance. Our COS renormalization prescription takes into account the 38% branching fraction of D^{*0} into $D^0\pi^0$ and the significant branching fraction of $X(3872)$ into decay modes other than $D^0\bar{D}^0\pi^0$. In original XEFT, there was a serious limitation on the precision from the need to truncate the expansion in m/M in order to avoid ultraviolet divergences. Our Galilean-invariant formulation makes this expansion unnecessary. The expansion may still be useful to obtain simple results, but it can be carried out to whatever order is required for the desired precision.

XEFT was invented to allow the effects of pion transitions on the $X(3872)$ resonance to be taken into account systematically. XEFT can also be used as a framework for quantifying the effects of physics beyond the $D\bar{D}\pi$ sector. This physics include charmonium states such as the $\chi_{c1}(2P)$, which couples to $D^*\bar{D}$, and $\psi(3770)$, which couples to $D\bar{D}$. It also includes tetraquark $c\bar{c}$ mesons and hybrid $c\bar{c}$ mesons. The improved precision of Galilean-invariant XEFT increases the motivation for using this effective field theory to quantify the effects of physics beyond the $D\bar{D}\pi$ sector.

Acknowledgments

This research was supported in part by the Department of Energy under grant DE-SC0011726 and by the Simons Foundation. I thank Hans-Werner Hammer for useful comments.

Appendix A: Loop Integrals

In this Appendix, we evaluate the loop integrals that are required to calculate the NLO transition amplitude using dimensional regularization. We also determine their poles in $d - 2$ and $d - 3$, where d is the number of spatial dimensions.

1. Reduction to momentum integrals

The loop integrals have D^* , D , and π propagators. Every loop has a D propagator, and it is convenient to take its energy and momentum to be the loop integration variables. A D propagator has a denominator of the form $p_0 - p^2/(2M) + i\epsilon$. The integral over p_0 can be evaluated by closing the contour around the pole at $p_0 = p^2/(2M)$, which puts the D on its energy shell. With dimensional regularization in d spatial dimensions, the measure for a momentum integral is

$$\int_{\mathbf{p}} \equiv \Lambda^{3-d} \int \frac{d^d p}{(2\pi)^d}, \quad (\text{A1})$$

where Λ is the renormalization scale. Tensor reduction can be used to reduce the loop momentum integrals to scalar integrals. Whenever possible, it is best to express the momentum-dependent terms in the numerator as a linear combination of the propagator denominators. After canceling terms in the numerator with propagators, the loop integrand reduces to a product of propagators.

The propagators in the loop integrand depend on the complex D^{*0} energy E_* and on the masses m and M of the π^0 and D^0 . The loop integrals depend on the masses through the reduced $D^*\bar{D}$ kinetic mass μ defined in Eq. (3a) and the reduced $D\pi$ mass μ_π defined in Eq. (3b). It is convenient to express the dependence on the masses in terms of μ and the ratio $r = \mu_\pi/\mu$ defined in Eq. (4).

In loop integrals that have cuts with $D\bar{D}\pi$ intermediate states, after integrating over the D and \bar{D} energies, the pion propagator depends on the momenta \mathbf{p} and \mathbf{q} of the D and \bar{D} and on the masses m and M . In evaluating the loop integral, it is often convenient to express the pion propagator in a form that depends on reduced masses instead of masses:

$$\begin{aligned} & \frac{i}{E - (\mathbf{p} + \mathbf{q})^2/(2m) - (p^2 + q^2)/(2M) + i\epsilon} \\ &= \frac{i}{E - (\mathbf{q} + \sqrt{1-r}\mathbf{p})^2/(2\mu_\pi) - p^2/(2\mu) + i\epsilon}. \end{aligned} \quad (\text{A2})$$

Unlike the first expression for the pion propagator in Eq. (A2), the second expression is not manifestly invariant under the interchange $\mathbf{p} \leftrightarrow \mathbf{q}$.

2. One-loop momentum integrals

The one-loop momentum integrals whose integrands are a D^* propagator raised to an integer power have the form

$$J_n(E) = \int_{\mathbf{p}} \frac{1}{[p^2 - 2\mu(E - E_*)]^n}. \quad (\text{A3})$$

The analytic result for this integral is

$$J_n(E) = \frac{\Lambda^{3-d}\Gamma(n-d/2)}{(4\pi)^{d/2}} [2\mu(E_* - E)]^{d/2-n}. \quad (\text{A4})$$

The branch cut in E is determined by the negative imaginary part of the complex energy E_* .

The one-loop momentum integrals whose integrands are a π propagator raised to an integer power have the form

$$I_n(E) = \int_{\mathbf{p}} \frac{1}{[p^2 - 2\mu_\pi E - i\epsilon]^n}. \quad (\text{A5})$$

The analytic result for this integral is

$$I_n(E) = r^{d/2-n} \frac{\Lambda^{3-d}\Gamma(n-d/2)}{(4\pi)^{d/2}} [e^{-i\pi} 2\mu E]^{d/2-n}. \quad (\text{A6})$$

where $r = \mu_\pi/\mu$ is the ratio of the reduced masses defined in Eq. (4). The branch cut in E is specified by the $i\epsilon$ prescription in Eq. (A5). Since we choose the zero of energy to be at the $D^0\bar{D}^0\pi^0$ threshold, we need only consider positive values for the real part of E .

The one-loop momentum integrals whose integrands have a single π propagator and a D^* propagator raised to an integer power are

$$L_n(E, p) = \int_{\mathbf{q}} \frac{1}{[q^2 - 2\mu(E - E_*)]^n} \frac{(2\mu)^{-1}}{(\mathbf{p} + \mathbf{q})^2/(2m) + (p^2 + q^2)/(2M) - E - i\epsilon}. \quad (\text{A7})$$

The function L_0 can be expressed in terms of the integral I_1 given by Eq. (A6):

$$L_0(E, p) = r I_1(E - p^2/2\mu). \quad (\text{A8})$$

This result can be obtained most easily by using the expression for the pion propagator on the right side of Eq. (A2), and then shifting the integration variable \mathbf{q} . The function L_1 can be expressed as a Feynman parameter integral:

$$\begin{aligned} L_1(E, p) &= r^{-d/2} \frac{\Lambda^{3-d}\Gamma(2-d/2)}{(4\pi)^{d/2}} \int_0^1 dx (x + (1-x)r)^2 \\ &\quad \times [-2(x + (1-x)r)\mu(E - (1-x)E_*) + xp^2]^{d/2-2}. \end{aligned} \quad (\text{A9})$$

We will need the expansions of these functions to first order in p^2 :

$$L_0(E, p) = rI_1(E) \left[1 - \frac{(d-2)p^2}{4\mu E} \right] + \mathcal{O}(p^4), \quad (\text{A10a})$$

$$\begin{aligned} L_1(E, p) &= \frac{J_1(E) - I_1(E)}{2\mu\Delta} \left[1 + \frac{r[4r(1-r)E + (4-4r-d)\Delta]p^2}{2d\mu\Delta^2} \right] \\ &\quad - \frac{r(d-2)[4(1-r)E - d\Delta]I_1(E)p^2}{8d\mu^2 E \Delta^2} + \mathcal{O}(p^4), \end{aligned} \quad (\text{A10b})$$

where $\Delta = (1-r)E - E_*$. The expansion for L_0 can be obtained most easily by expanding the expression in Eq. (A8) in powers of p^2 . The expansion for L_1 can be obtained most easily by expanding the integrand in Eq. (A7) in powers of \mathbf{p} and averaging over angles to reduce it to scalar integrals. The scalar integrals can be expressed in terms of the integrals J_n and I_n given by Eqs. (A4) and (A6). They can all be reduced algebraically to J_1 and I_1 .

3. Two-loop momentum integrals

The two-loop momentum integrals whose integrands have a π propagator and one or two D^* propagators raised to integer powers are

$$\begin{aligned} K_{lmn}(E) &= \int_{\mathbf{p}} \int_{\mathbf{q}} \frac{1}{[p^2 - 2\mu(E - E_*)]^m [q^2 - 2\mu(E - E_*)]^n} \\ &\quad \times \frac{(2\mu)^{-l}}{[(\mathbf{p} + \mathbf{q})^2/(2m) + (p^2 + q^2)/(2M) - E - i\epsilon]^l}. \end{aligned} \quad (\text{A11})$$

The momentum integrals with a π propagator and a single D^* propagator can be expressed as integrals over a single Feynman parameter:

$$K_{110}(E) = r^{d/2} \frac{\Lambda^{6-2d}\Gamma(2-d)}{(4\pi)^d} \int_0^1 dx (1-x)^{-d/2} [2\mu(xE_* - E)]^{d-2}, \quad (\text{A12a})$$

$$K_{120}(E) = r^{d/2} \frac{\Lambda^{6-2d}\Gamma(3-d)}{(4\pi)^d} \int_0^1 dx x(1-x)^{-d/2} [2\mu(xE_* - E)]^{d-3}, \quad (\text{A12b})$$

where $r = \mu_\pi/\mu$. The momentum integrals with a π propagator and two D^* propagators can be expressed as an integral over two Feynman parameters:

$$\begin{aligned} K_{111}(E) &= r^{d/2} \frac{\Lambda^{6-2d}\Gamma(3-d)}{(4\pi)^d} \int_0^1 dw w [2\mu(wE_* - E)]^{d-3} \\ &\quad \times \int_0^1 dt [1-w + rw^2t(1-t)]^{-d/2}. \end{aligned} \quad (\text{A13})$$

This function depends on r through the prefactor $r^{d/2}$ and through the integral over t . For a given dimension d , $K_{111}(E)$ can be expanded in powers of r . The expansion is not straightforward, because there are negative powers of r that arise from the $w \rightarrow 1$ endpoint region.

4. Poles in $d - 2$

In a dimensionally regularized loop integral, poles in $d - 2$ are associated with linear ultraviolet (UV) divergences in 3 spatial dimensions. An UV pole in $d - 2$ can arise from a factor of $\Gamma(1 - d/2)$ or $\Gamma(2 - d)$ obtained by integrating over a loop momentum. In the two-loop momentum integrals K_{110} and K_{120} defined in Eqs. (A12), the integral over the Feynman parameter x also gives an UV pole in $d - 2$.

The one-loop momentum integrals J_1 and I_1 given by Eqs. (A4) and (A6) have single poles in $d - 2$. We will need the pole and the constant term:

$$J_1(E) \longrightarrow -\frac{\Lambda}{2\pi} \left[\frac{1}{d-2} + \frac{1}{2} \log \frac{2\mu(E_* - E)}{\Lambda^2} \right], \quad (\text{A14a})$$

$$I_1(E) \longrightarrow -\frac{\Lambda}{2\pi} \left[\frac{1}{d-2} + \frac{1}{2} \left(\log \frac{2\mu E}{\Lambda^2} + \log r - i\pi \right) \right]. \quad (\text{A14b})$$

The momentum scale $\bar{\Lambda}$ in the logarithms is

$$\bar{\Lambda} = \sqrt{4\pi} e^{-\gamma/2} \Lambda, \quad (\text{A15})$$

where γ is Euler's constant. We will need the constant term in the integral J_2 given by Eq. (A4):

$$J_2(E) \longrightarrow \frac{\Lambda}{8\pi\mu(E_* - E)}. \quad (\text{A16})$$

We will also need the pole term in the integral L_0 in Eq. (A8):

$$L_0(E, p) \longrightarrow -\frac{r\Lambda}{2\pi(d-2)}. \quad (\text{A17})$$

The two-loop momentum integral K_{110} defined in Eq. (A12a) has a double and single pole in $d-2$, while K_{120} defined in Eq. (A12b) has only a single pole:

$$K_{110}(E) \longrightarrow \frac{2r\Lambda^2}{(4\pi)^2} \left[\frac{1}{(d-2)^2} + \frac{1}{d-2} \left(\log \frac{-2\mu(E - E_*)}{\bar{\Lambda}^2} + \frac{1}{2} \log r \right) \right], \quad (\text{A18a})$$

$$K_{120}(E) \longrightarrow \frac{r\Lambda^2}{(4\pi)^2(d-2)\mu(E - E_*)}. \quad (\text{A18b})$$

5. Integrals at the $D^{*0}\bar{D}^0$ threshold

If the one-loop integral $J_n(E)$ given by Eq. (A4) is analytically continued to $d=3$ and then evaluated at $E=E_*$, it has an infrared divergence for $n \geq 3/2$. However if it is evaluated at $E=E_*$ and then analytically continued to $d=3$, it vanishes because the integral has no momentum scale:

$$J_n(E_*) = 0, \quad (\text{A19})$$

The two-loop integrals $K_{lmn}(E)$ defined in Eq. (A11) can be evaluated analytically at the threshold $E=E_*$. The integrals $K_{110}(E_*)$, $K_{120}(E_*)$, and $K_{111}(E_*)$ each has a single pole in $d-3$. Their values near $d=3$, including the pole in $d-3$ and the finite term, are

$$K_{110}(E_*) = \frac{(-2)r^{3/2}(2\mu E_*)}{(4\pi)^3} \left(\frac{1}{d-3} - 2 + \frac{1}{2} \log r + \log \frac{2\mu E_*}{\bar{\Lambda}^2} - i\pi \right), \quad (\text{A20a})$$

$$K_{120}(E_*) = \frac{4r^{3/2}}{(4\pi)^3} \left(\frac{1}{d-3} + \frac{1}{2} \log r + \log \frac{2\mu E_*}{\bar{\Lambda}^2} - i\pi \right), \quad (\text{A20b})$$

$$K_{111}(E_*) = \frac{(-4)r}{(4\pi)^3} \left[\frac{\arccos(\sqrt{r})}{\sqrt{1-r}} \left(\frac{1}{d-3} - 2 + \log r + \log \frac{2\mu E_*}{\bar{\Lambda}^2} - i\pi \right) \right. \\ \left. + \frac{d}{dd} {}_2F_1\left(\frac{1}{2}d-1, \frac{1}{2}d-1, \frac{1}{2}d; 1-r\right) \Big|_{d=3} \right]. \quad (\text{A20c})$$

The momentum scale $\bar{\Lambda}$ in the logarithms is defined in Eq. (A15). The pole in $K_{110}(E_*)$ is the sum of an UV pole and an infrared pole in $d-3$.

6. Integrals near $d=3$

The one-loop integrals J_1 and J_2 at $d=3$ are

$$J_1(E) = -\frac{1}{4\pi} [2\mu(E_* - E)]^{1/2}, \quad (\text{A21a})$$

$$J_2(E) = -\frac{1}{8\pi} [2\mu(E_* - E)]^{-1/2}. \quad (\text{A21b})$$

The one-loop integrals I_1 and I_2 at $d = 3$ are

$$I_1(E) = ir^{1/2} \frac{1}{4\pi} [2\mu E]^{1/2}, \quad (\text{A22a})$$

$$I_2(E) = -ir^{-1/2} \frac{1}{8\pi} [2\mu E]^{-1/2}. \quad (\text{A22b})$$

The two-loop momentum integrals $K_{lmn}(E)$ near $d = 3$ are expressed in terms of Feynman parameter integrals in Eqs. (A12) and (A13). In order to obtain expressions for these functions near $d - 3$, it is necessary to make subtractions of the integrands to make them integrable at $x = 1$. The resulting expression for $K_{110}(E)$, including the pole in $d - 3$ and the finite term, is

$$\begin{aligned} K_{110}(E) = & \frac{4r^{3/2}\mu}{(4\pi)^3} \left[\left(\frac{1}{d-3} - 2 + \frac{1}{2} \log r + \log \frac{2\mu(E-E_*)}{\Lambda^2} - i\pi \right) (E-2E_*) \right. \\ & \left. - 2E_* - \frac{1}{2} \int_0^1 dx (1-x)^{-3/2} (E-xE_*) \log \frac{E-xE_*}{E-E_*} \right]. \end{aligned} \quad (\text{A23})$$

The pole with its residue evaluated at $E = E_*$ is also the UV pole in $d - 3$ of $K(E_*)$. The difference between the pole of $K(E_*)$ in Eq. (A20a) and this pole is the infrared pole in $d - 3$ of $K(E_*)$. The UV poles in $d - 3$ of $K_{120}(E)$ and $K_{111}(E)$ are the same as the poles in their values at E_* given in Eqs. (A20b) and (A20c). The differences between their values at E in Eqs. (A12b) and (A12b) and their values at E_* are finite:

$$K_{120}(E) = K_{120}(E_*) + \frac{4r^{3/2}}{(4\pi)^3} \left[\log \frac{E-E_*}{E_*} - \frac{1}{4} \int_0^1 dx x(1-x)^{-3/2} \log \frac{E-xE_*}{E-E_*} \right], \quad (\text{A24a})$$

$$K_{111}(E) = K_{111}(E_*) - \frac{r^{3/2}}{(4\pi)^3} \int_0^1 dw \frac{w}{\sqrt{1-w}(1-w+rw^2/4)} \log \frac{E-wE_*}{(1-w)E_*}. \quad (\text{A24b})$$

7. Threshold expansions

Threshold expansions for the two-loop integrals $K_{lmn}(E)$ near $d = 3$ cannot be obtained simply by expanding the expressions in Eqs. (A23), (A24a), and (A24b) in powers of $E - E_*$, because this generates infrared divergences in the Feynman parameter integrals. The threshold expansion for $K_{111}(E)$ for general d can be obtained in a straightforward way by expanding the defining integral in Eq. (A11) in powers of $E - E_*$. The expansion through second order in $E - E_*$ is

$$\begin{aligned} K_{111}(E) = & K_{111}(E_*) + [K_{211}(E_*) + 2K_{121}(E_*)] 2\mu(E-E_*) \\ & + [K_{311}(E_*) + 2K_{221}(E_*) + K_{122}(E_*) + 2K_{131}(E_*)] [2\mu(E-E_*)]^2 \\ & + \mathcal{O}((E-E_*)^3). \end{aligned} \quad (\text{A25})$$

The reason the threshold expansion of $K_{111}(E)$ is straightforward is that the only momentum region that contributes is where both loop momenta are of order $(\mu|E_*|)^{1/2}$.

In contrast, the integrals $K_{110}(E)$ and $K_{120}(E)$ have contributions from regions where one loop momentum is of order $(\mu|E - E_*|)^{1/2}$. These contributions have an expansion in non-integer powers of $E - E_*$. By inserting the alternative expression for the pion propagator in Eq. (A2) into the defining integral for $K_{lm0}(E)$ in Eq. (A11) and then shifting the momentum \mathbf{q} , it can be expressed as

$$K_{lm0}(E) = r^l \int_{\mathbf{p}} \frac{1}{[p^2 - 2\mu(E-E_*)]^m} \int_{\mathbf{q}} \frac{1}{[q^2 - 2\mu E_* + r(p^2 - 2\mu(E-E_*)) - i\epsilon]^l}. \quad (\text{A26})$$

The expansion of the pion propagator in powers of $p^2 - 2\mu(E - E_*)$ produces a sum of products of one-loop integrals of the form $I_{l+k}(E_*)J_{m-k}(E)$. With dimensional regularization, the terms with $k \geq m$ are zero because the integral over \mathbf{p} has no scale. The threshold expansion for $K_{lm0}(E)$ is the sum of the terms with the noninteger powers

$(E - E_*)^{d/2-m+k}$ and the terms with integer powers that can be obtained by expanding the integrand of Eq. (A26) in powers of $E - E_*$. The expansions of $K_{110}(E)$ and $K_{120}(E)$ through second order in $E - E_*$ are

$$\begin{aligned} K_{110}(E) &= K_{110}(E_*) + rI_1(E_*)J_1(E) + [K_{210}(E_*) + K_{120}(E_*)]2\mu(E - E_*) \\ &\quad + [K_{310}(E_*) + K_{220}(E_*) + K_{130}(E_*)][2\mu(E - E_*)]^2 + \mathcal{O}((E - E_*)^3), \end{aligned} \quad (\text{A27a})$$

$$\begin{aligned} K_{120}(E) &= K_{120}(E_*) + rI_1(E_*)J_2(E) - r^2I_2(E_*)J_1(E) + [K_{220}(E_*) + 2K_{130}(E_*)]2\mu(E - E_*) \\ &\quad + [K_{320}(E_*) + 2K_{230}(E_*) + 3K_{140}(E_*)][2\mu(E - E_*)]^2 + \mathcal{O}((E - E_*)^3). \end{aligned} \quad (\text{A27b})$$

The integer powers of $E - E_*$ in the threshold expansions in Eqs. (A25) and (A27) are determined by the two-loop integrals $K_{lmn}(E_*)$. By inserting the alternative expression for the pion propagator in Eq. (A2) into the defining integral for $K_{lmn}(E)$ in Eq. (A11), its value at the threshold $E = E_*$ reduces to

$$K_{lmn}(E_*) = r^l \int_{\mathbf{p}} \frac{1}{[p^2]^m} \int_{\mathbf{q}} \frac{1}{[q^2]^n [(q + \sqrt{1-r}\mathbf{p})^2 + rp^2 - 2r\mu E_* - i\epsilon]^l}. \quad (\text{A28})$$

The denominators of the integral over \mathbf{q} can be combined by introducing a Feynman parameter. After evaluating the integral over \mathbf{q} , the integral over \mathbf{p} can also be evaluated analytically. The integral over the Feynman parameter gives a hypergeometric function;

$$\begin{aligned} K_{lmn}(E_*) &= \frac{r^{d-m-n}}{(4\pi)^3} \left(\frac{1}{4\pi\Lambda^2} \right)^{d-3} \frac{\Gamma(l+m+n-d)\Gamma(d/2-m)\Gamma(d/2-n)}{\Gamma(l)\Gamma^2(d/2)} \\ &\quad \times {}_2F_1(d/2-m, d/2-n, d/2, 1-r) [e^{-i\pi} 2\mu E_*]^{d-l-m-n}. \end{aligned} \quad (\text{A29})$$

If $n = 0$, the hypergeometric function reduces to $r^{m-d/2}$. Inserting the expression for $K_{lmn}(E_*)$ in Eq.(A29) into Eqs. (A27a), (A27b), and (A25), the threshold expansions through second order in $E - E_*$ are

$$\begin{aligned} K_{110}(E) &= K_{110}(E_*) + rI_1(E_*)J_1(E) \\ &\quad + \frac{2r^{3/2}(2\mu E_*)}{(4\pi)^3} \left(\frac{1}{d-3} + 1 + \frac{1}{2} \log r + \log \frac{2\mu E_*}{\Lambda^2} - i\pi \right) \frac{E_* - E}{E_*} \\ &\quad + \frac{r^{3/2}(2\mu E_*)}{3(4\pi)^3} \left(\frac{E_* - E}{E_*} \right)^2 + \mathcal{O}((E - E_*)^3), \end{aligned} \quad (\text{A30a})$$

$$\begin{aligned} K_{120}(E) &= K_{120}(E_*) + rI_1(E_*)J_2(E) - r^2I_2(E_*)J_1(E) \\ &\quad - \frac{4r^{3/2}}{3(4\pi)^3} \frac{E_* - E}{E_*} + \frac{2r^{3/2}}{15(4\pi)^3} \left(\frac{E_* - E}{E_*} \right)^2 + \mathcal{O}((E - E_*)^3), \end{aligned} \quad (\text{A30b})$$

$$\begin{aligned} K_{111}(E) &= K_{111}(E_*) + \frac{4}{(4\pi)^3} \left((2-r) \frac{\arccos(\sqrt{r})}{\sqrt{1-r}} + 2\sqrt{r} \right) \frac{E_* - E}{E_*} \\ &\quad + \frac{2r^{-1}}{(4\pi)^3} \left((2-4r+r^2) \frac{\arccos(\sqrt{r})}{\sqrt{1-r}} + \frac{2(3-4r)}{3} \sqrt{r} \right. \\ &\quad \left. + 8 {}_2F_1(-\frac{1}{2}, -\frac{1}{2}, \frac{3}{2}, 1-r) \right) \left(\frac{E_* - E}{E_*} \right)^2 + \mathcal{O}((E - E_*)^3). \end{aligned} \quad (\text{A30c})$$

The function $\arccos(\sqrt{r})$ in Eq. (A30c) has an expansion in odd powers of $r^{1/2}$:

$$\arccos(\sqrt{r}) = \frac{\pi}{2} \left(1 - \frac{2}{\pi} r^{1/2} - \frac{1}{3\pi} r^{3/2} + \dots \right). \quad (\text{A31})$$

The hypergeometric function in Eq. (A30c) has an expansion in powers of r :

$${}_2F_1(-\frac{1}{2}, -\frac{1}{2}, \frac{3}{2}, 1-r) = \frac{3\pi}{8} \left(1 - \frac{1}{6}r + \frac{1}{24}r^2 + \dots \right). \quad (\text{A32})$$

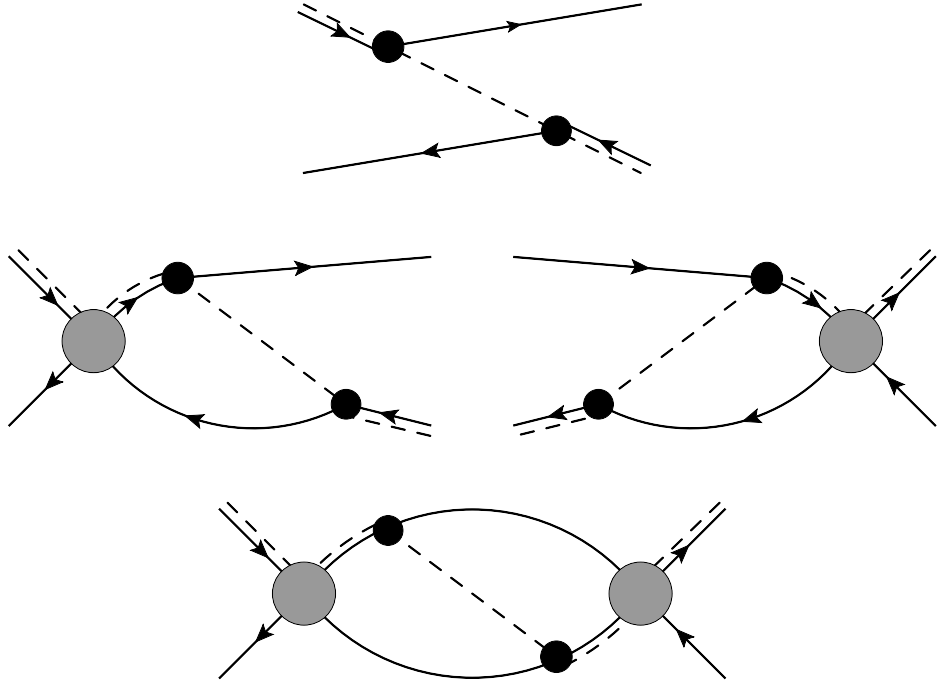


FIG. 9: Pion-exchange diagrams for $D^{*0}\bar{D}^0 \rightarrow D^{*0}\bar{D}^0$. They consist of the tree diagram $A1$, the one-loop diagrams $A2$ and $A3$ in which either the incoming or the outgoing charm mesons interact through a LO transition amplitude, and the two-loop diagram $A4$ in which they both interact through LO transition amplitudes. The absence of arrows on the charm mesons lines in the diagram $A4$ implies a sum over the two possible directions of the arrows.

Appendix B: Diagrams for NLO Transition Amplitude

In this Appendix, we give results for the individual diagrams that contribute to the transition amplitude $+i\mathcal{A}^{ij}/2$ for $D^{*0}\bar{D}^0 \rightarrow D^{*0}\bar{D}^0$ in the $C = +$ channel, with the external legs amputated and the initial and final \bar{D}^0 on their energy shells. In the center-of-momentum frame, the amplitude $\mathcal{A}^{ij}(E, \mathbf{p}, \mathbf{p}')$ is a function of the total energy E and the relative momenta \mathbf{p} and \mathbf{p}' of the incoming and outgoing charm mesons, respectively. The LO amplitude is the solution to the Lippmann-Schwinger integral equation shown in Figure 8. The amplitude at NLO can be expressed as

$$\mathcal{A}^{ij}(E, \mathbf{p}, \mathbf{p}') = (2\pi/\mu)\mathcal{A}(E)\delta^{ij} + \sum_n \mathcal{A}_n^{ij}(E, \mathbf{p}, \mathbf{p}'), \quad (B1)$$

where the sum is over the NLO diagrams and the amplitude $\mathcal{A}(E)$ in the LO term is

$$\mathcal{A}(E) = \frac{\mu/(2\pi)}{-C_0^{-1} - 2\mu J_1(E)}. \quad (B2)$$

The one-loop momentum integral J_1 is given in Eq. (A4). In the physical dimension $d = 3$, the amplitude $\mathcal{A}(E)$ reduces to the expression in Eq. (39). The NLO diagrams for the transition amplitude can be organized into five sets of 4 diagrams labeled A , B , C , and D .

1. Pion-exchange diagrams

There are four diagrams that involve the emission of a pion by D^{*0} and its absorption by \bar{D}^0 . The four pion-exchange diagrams, which are labelled $A1$, $A2$, $A3$, and $A4$, are shown in Fig. 9. The amplitude for the tree diagram $A1$ is a tensor in the vector indices i and j that depends on the relative momenta \mathbf{p}' and \mathbf{p} :

$$\begin{aligned} \mathcal{A}_{A1}^{ij}(E, \mathbf{p}, \mathbf{p}') = & \left(\frac{g^2}{4m f_\pi^2} \right) \frac{-2}{E - (p^2 + p'^2)/(2M) - (\mathbf{p} + \mathbf{p}')^2/(2m) + i\epsilon} \\ & \times \left(\frac{M}{M+m} \mathbf{p} + \mathbf{p}' \right)^i \left(\frac{M}{M+m} \mathbf{p}' + \mathbf{p} \right)^j. \end{aligned} \quad (B3)$$

This can be expressed in a form that depends on the masses only though reduced masses:

$$\mathcal{A}_{A1}^{ij}(E, \mathbf{p}, \mathbf{p}') = \left(\frac{g^2}{4m f_\pi^2} \right) \frac{(-2)(\sqrt{1-r}\mathbf{p} + \mathbf{p}')^i (\sqrt{1-r}\mathbf{p}' + \mathbf{p})^j}{E - p^2/(2\mu) - (\mathbf{p}' + \sqrt{1-r}\mathbf{p})^2/(2\mu_\pi) + i\epsilon}, \quad (\text{B4})$$

where $r = \mu_\pi/\mu$. Unlike the expression in Eq. (B3), the expression in Eq. (B4) is not manifestly invariant under the simultaneous interchanges $\mathbf{p} \leftrightarrow \mathbf{p}'$ and $i \leftrightarrow j$. The amplitude for the diagram $A1$ vanishes in the zero-momentum limit $\mathbf{p}, \mathbf{p}' \rightarrow 0$.

The amplitudes for the one-loop diagrams $A2$ and $A3$ in Fig. 9 are tensors in the indices i and j that depend on the relative momenta \mathbf{p}' and \mathbf{p} , respectively. They can be decomposed into transverse and longitudinal components. The Feynman rule for the LO transition amplitude is given in Eq. (44). The amplitudes for the diagrams $A3$ and $A2$ are

$$\begin{aligned} \mathcal{A}_{A3}^{ij}(E, \mathbf{p}) &= \left(\frac{g^2}{4m f_\pi^2} \right) \frac{4\pi\mu^2}{(d-1)\sqrt{1-r}p^2} \mathcal{A}(E) \\ &\times \left\{ \left[-(\Delta(E, p) + rp^2/\mu)L_0(E, p) - 2\mu(\Delta(E, p)^2 - 2rE_*p^2/\mu)L_1(E, p) \right. \right. \\ &\quad \left. \left. + r(\Delta(E, p) + p^2/\mu)J_1(E) \right] (\delta^{ij} - p^i p^j / p^2) \right. \\ &\quad \left. + (d-1)[\Delta(E, p)L_0(E, p) + 2\mu\Delta(E, p)(\Delta(E, p) + rp^2/\mu)L_1(E, p) \right. \\ &\quad \left. \left. - r(\Delta(E, p) - (1-r)p^2/\mu)J_1(E)] p^i p^j / p^2 \right\}, \right. \end{aligned} \quad (\text{B5a})$$

$$\mathcal{A}_{A2}^{ij}(E, \mathbf{p}') = \mathcal{A}_{A3}^{ij}(E, \mathbf{p} \rightarrow \mathbf{p}'). \quad (\text{B5b})$$

The one-loop integrals J_1 , L_0 , and L_1 are given by Eqs. (A4), (A8), and (A9), and Δ is a linear function of E and p^2 :

$$\Delta(E, p) = (1-r)E - E_* - p^2/(2\mu). \quad (\text{B6})$$

The expression for the amplitude $\mathcal{A}_{A3}^{ij}(E, \mathbf{p})$ in Eq. (B5a) has terms proportional to δ^{ij}/p^2 , $p^i p^j/p^4$, and $p^i p^j/p^2$ that are not analytic functions of the momentum vector \mathbf{p} in the neighborhood of $\mathbf{p} = 0$. The limit $\mathbf{p} \rightarrow 0$ can be obtained by using the expansions for $L_0(E, p)$ and $L_1(E, p)$ to first order in p^2 given in Eqs. (A10). The nonanalytic terms cancel in the limit $\mathbf{p} \rightarrow 0$. The diagram $A2$ has the same zero-momentum limit. The sum of the amplitudes for the diagrams $A2$ and $A3$ in the zero-momentum limit is

$$\mathcal{A}_{A2+A3}^{ij}(E, 0) = \left(\frac{g^2}{4m f_\pi^2} \right) \frac{16\pi r \sqrt{1-r} \mu [(E - E_*)J_1(E) - rEI_1(E)]}{d[(1-r)E - E_*]} \mathcal{A}(E) \delta^{ij}. \quad (\text{B7})$$

The one-loop integral I_1 is given in Eq. (A6).

The two-loop diagram $A4$ in Fig. 9 is the sum of a diagram in which a pion is emitted by D^{*0} and absorbed by \bar{D}^0 and a diagram in which a pion is emitted by \bar{D}^{*0} and absorbed by D^0 . The amplitude for this diagram is diagonal in the vector indices i and j and depends only on E :

$$\begin{aligned} \mathcal{A}_{A4}^{ij}(E) &= \left(\frac{g^2}{4m f_\pi^2} \right) \frac{(-16\pi^2)r\mu}{d\sqrt{1-r}} [2K_{110}(E) - 2\mu(2E_* - rE)K_{111}(E) \\ &\quad -(2-r)J_1(E)^2] \mathcal{A}^2(E) \delta^{ij}. \end{aligned} \quad (\text{B8})$$

The two-loop integrals K_{110} and K_{111} are given in Eqs. (A12a) and (A13).

2. D^* propagator correction diagrams

There are two NLO diagrams involving a correction to a D^* propagator. The two diagrams, which are labelled $B1$ and $B2$, are shown in Figure 10. The diagram $B1$ has a D^* self-energy subdiagram inserted into the D^* propagator. It can be reduced to

$$\mathcal{A}_{B1}^{ij}(E) = \left(\frac{g^2}{4m f_\pi^2} \right) \frac{(-32\pi^2)r\mu}{d} [K_{110}(E) - 2\mu E_* K_{120}(E)] \mathcal{A}^2(E) \delta^{ij}. \quad (\text{B9})$$

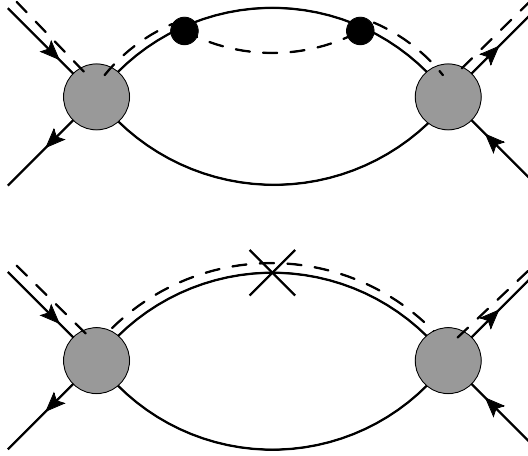


FIG. 10: D^* propagator correction diagrams for $D^{*0}\bar{D}^0 \rightarrow D^{*0}\bar{D}^0$. The two-loop diagram $B1$ has a D^* self-energy subdiagram inserted into the D^* propagator. The one-loop diagram $B2$ has a D^* self-energy counterterm inserted into the D^* propagator.

The two-loop integrals K_{110} and K_{120} are given in Eqs. (A12). The diagram $B2$ has a D^* propagator counterterm inserted into the D^* propagator. The Feynman rule for the self-energy counterterm is given in Eq. (31). With the complex on-shell renormalization scheme for the D^{*0} propagator, the diagram $B2$ can be reduced to

$$\mathcal{A}_{B2}^{ij}(E) = \left(\frac{g^2}{4m f_\pi^2} \right) \frac{(-16\pi^2)r^2\mu}{d} I_1(E_*) [4\mu E_* J_2(E) - dJ_1(E)] \mathcal{A}^2(E) \delta^{ij}. \quad (\text{B10})$$

The one-loop integrals J_n are given in Eq. (A4).

3. ∇^2 vertex diagrams

There are four NLO diagrams with a ∇^2 vertex. The four diagrams, which are labelled $C1$, $C2$, $C3$, and $C4$, are shown in Fig. 11. The amplitude for the first diagram $C1$ is just the ∇^2 vertex in Eq. (15):

$$\mathcal{A}_{C1}^{ij}(E, p, p') = (-C_2/2) (p^2 + p'^2) \delta^{ij}. \quad (\text{B11})$$

The factor of $p^2 + p'^2$ depends on the relative momenta of the incoming and outgoing charm mesons. If there is a contact interaction between the incoming charm mesons, p is replaced by a loop momentum k . The amplitude for the diagram $C2$ in which the incoming charm mesons interact through a LO transition amplitude can be obtained from Eq. (B11) by multiplying it by $(4\pi/\mu)J_1(E)\mathcal{A}(E)$ and replacing p^2 by the loop-integral-weighted average of k^2 :

$$\mathcal{A}_{C2}^{ij}(E, p') = -2\pi C_2 J_1(E) \mathcal{A}(E) (\langle k^2 \rangle + p'^2) \delta^{ij}. \quad (\text{B12})$$

The loop-integral-weighted average of k^2 is defined by

$$\langle k^2 \rangle = \frac{\int_k k^2/[E - E_* - k^2/(2\mu)]}{\int_k 1/[E - E_* - k^2/(2\mu)]}. \quad (\text{B13})$$

With dimensional regularization, the loop-integral-weighted average is very simple:

$$\langle k^2 \rangle = 2\mu(E - E_*). \quad (\text{B14})$$

The amplitude for the diagram $C3$ is obtained from Eq. (B12) by replacing p' by p . The amplitude for the diagram $C4$ is

$$\mathcal{A}_{C4}^{ij}(E) = -16\pi^2 C_2 J_1(E)^2 \mathcal{A}^2(E) \langle k^2 \rangle \delta^{ij}. \quad (\text{B15})$$

The sum of the four diagrams $C1$, $C2$, $C3$, and $C4$ has a multiplicative factor $1 + 4\pi J_1 \mathcal{A}$ that can be simplified by using the expression for $A_0(E)$ in Eq. (B2):

$$\mathcal{A}_C^{ij}(E, p, p') = \frac{\pi C_2}{\mu C_0} [(p^2 + p'^2) \mathcal{A}(E) + 16\pi\mu(E - E_*) J_1(E) \mathcal{A}^2(E)] \delta^{ij}. \quad (\text{B16})$$

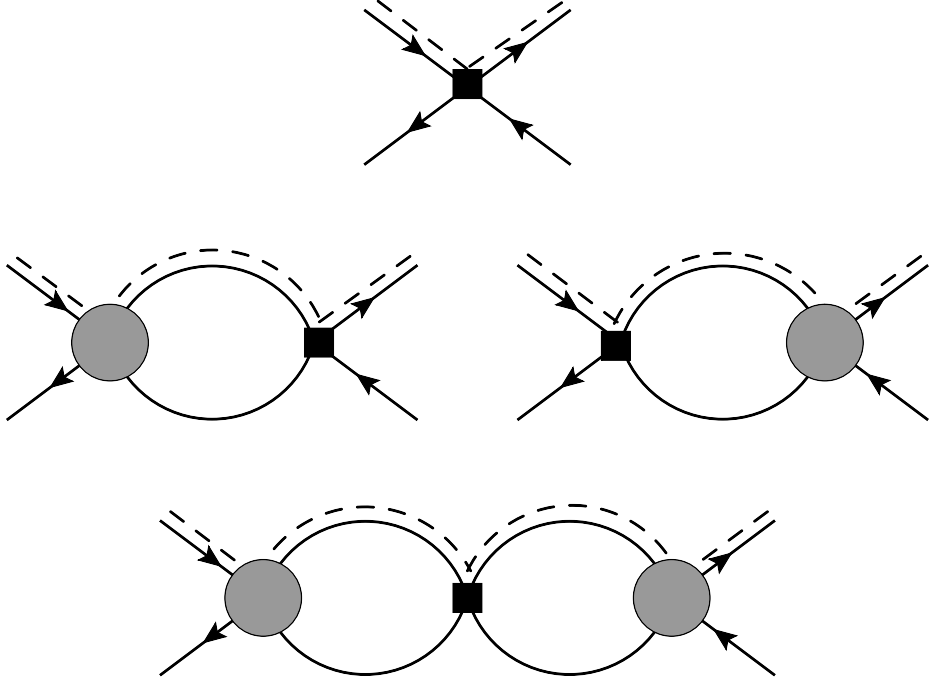


FIG. 11: The ∇^2 vertex diagrams for $D^{*0}\bar{D}^0 \rightarrow D^{*0}\bar{D}^0$. They consist of the ∇^2 vertex $C1$, the one-loop diagrams $C2$ and $C3$ in which either the incoming or the outgoing charm mesons interact through a LO transition amplitude, and the two-loop diagram $C4$ in which they both interact through LO transition amplitudes.

4. $D^*\bar{D}$ counterterm diagrams

There are four NLO diagrams that can be obtained from the diagrams in Figure 11 by replacing the ∇^2 vertex by a $D^*\bar{D}$ counterterm. The four diagrams are labelled $D1$, $D2$, $D3$, and $D4$. The amplitude for the diagram $D1$ is just the counterterm vertex in Eq. (16):

$$\mathcal{A}_{D1}^{ij} = -[\delta C_0 + \delta D_0 E] \delta^{ij}. \quad (\text{B17})$$

The amplitudes for the diagrams $D2$ and $D3$ each differs from this by a multiplicative factor $4\pi J_1 \mathcal{A}$. The amplitude for the diagram $D4$ differs by two such factors. The sum of the four diagrams $D1$, $D2$, $D3$, and $D4$ therefore has a factor $[1 + 4\pi J_1 \mathcal{A}]^2$ that can be simplified by using the expression for $A_0(E)$ in Eq. (B2):

$$\mathcal{A}_D^{ij}(E) = -\frac{4\pi^2 [\delta C_0 + \delta D_0 E]}{\mu^2 C_0^2} \mathcal{A}^2(E) \delta^{ij}. \quad (\text{B18})$$

The δC_0 term in this expression can also be obtained from the LO transition amplitude in Eq. (B2) by replacing C_0^{-1} by $C_0^{-1} - \delta C_0/C_0^2$ and expanding the amplitude to first order in δC_0 .

5. Complete NLO amplitude

The complete NLO term in the transition amplitude $\mathcal{A}^{ij}(E, \mathbf{p}, \mathbf{p}')$ is the sum of (A) the pion-exchange diagrams in Eqs. (B3), (B5), and (B8), (B) the D^* propagator insertion diagrams in Eqs. (B9) and (B10), (C) the ∇^2 vertex diagrams in Eqs. (B16), and (D) the $D^*\bar{D}$ counterterm diagrams in Eq. (B18). In the zero-momentum limit $\mathbf{p}, \mathbf{p}' \rightarrow 0$, the pion-exchange diagrams reduce to the sum of Eqs. (B7) and (B8) and the ∇^2 vertex diagrams in Eqs. (B16) reduce to the single term with the factor of $\mathcal{A}^2(E)$.

6. Poles in $d - 2$

The momentum integrals with poles in $d - 2$ are given in Section A 4. In the NLO term in the transition amplitude $\mathcal{A}^{ij}(E, \mathbf{p}, \mathbf{p}')$, all the terms with a double pole in $d - 2$ have the tensor structure δ^{ij} . All the terms with a single pole

in $d - 2$ also have the tensor structure δ^{ij} , with the exception of terms from the diagram $A3$ with the tensor structure $p^i p^j / p^2$ and terms from the diagram $A2$ with the tensor structure $p'^i p'^j / p'^2$. Upon using the identities $L_0 = rJ_1$ and $L_1 = 0$ for the pole terms, the diagram $A3$ in Eq. (B5a) reduces to

$$\mathcal{A}_{A3}^{ij}(E, \mathbf{p}) \longrightarrow \left(\frac{g^2}{4m f_\pi^2} \right) \frac{4\pi r \sqrt{1-r} \mu}{d-1} J_1 \mathcal{A}(E) [\delta^{ij} + (d-2)p^i p^j / p^2]. \quad (\text{B19})$$

Thus the single pole in $d - 2$ has the tensor structure δ^{ij} even at nonzero momentum.

We now consider the terms with the tensor structure δ^{ij} in the zero-momentum limit. The pion-exchange diagrams $A2$ and $A3$ in Eq. (B7) and the ∇^2 vertex diagrams C in Eq. (B16) have single poles in $d - 2$:

$$\mathcal{A}_{A2+A3}^{ij}(E, 0) \longrightarrow \left(\frac{g^2}{4m f_\pi^2} \right) \frac{(-4)r \sqrt{1-r} \mu \Lambda}{d-2} \mathcal{A}(E) \delta^{ij}, \quad (\text{B20a})$$

$$\mathcal{A}_C^{ij}(E, 0, 0) \longrightarrow \frac{8\pi C_2 \Lambda}{(d-2)C_0} (E_* - E) \mathcal{A}^2(E) \delta^{ij}. \quad (\text{B20b})$$

The two-loop pion-exchange diagram $A4$ in Eq. (B8) and the sum of the D^* propagator correction diagrams $B1$ and $B2$ in Eqs. (B9) and (B10) have double and single poles in $d - 2$:

$$\begin{aligned} \mathcal{A}_{A4}^{ij}(E) &\longrightarrow \left(\frac{g^2}{4m f_\pi^2} \right) 4r \sqrt{1-r} \mu \Lambda^2 \left[\frac{1}{(d-2)^2} \right. \\ &\quad \left. + \frac{1}{d-2} \left(\log \frac{2\mu(E_* - E)}{\Lambda^2} - \frac{r \log r}{4(1-r)} - \frac{1}{2} \right) \right] \mathcal{A}^2(E) \delta^{ij}, \end{aligned} \quad (\text{B21a})$$

$$\begin{aligned} \mathcal{A}_B^{ij}(E) &\longrightarrow \left(\frac{g^2}{4m f_\pi^2} \right) 2r^2 \mu \Lambda^2 \left[\frac{1}{(d-2)^2} \right. \\ &\quad \left. + \frac{1}{d-2} \left(\log \frac{2\mu E_*}{\Lambda^2} + \frac{1}{2} \log r + \frac{1}{2} - i\pi \right) \right] \mathcal{A}^2(E) \delta^{ij}. \end{aligned} \quad (\text{B21b})$$

7. Poles in $d - 3$

The only NLO diagrams for the transition amplitude that have poles in $d - 3$ are the two-loop pion-exchange diagram $A4$ in Eq. (B8) and the D^* self-energy insertion diagram $B1$ in Eq. (B9). The momentum integrals with poles in $d - 3$ are the two-loop integrals K_{110} , K_{120} , and K_{111} . The poles are given in Eqs. (A23), (A20b), and (A20c), respectively. The pole terms are

$$\begin{aligned} \mathcal{A}_{A4}^{ij}(E) &\longrightarrow \left(\frac{g^2}{4m f_\pi^2} \right) \frac{(-2)r^2 \mu^3}{3\pi(d-3)} \left[\frac{r^{1/2}}{\sqrt{1-r}} (E - 2E_*) \right. \\ &\quad \left. + \frac{\arccos(\sqrt{r})}{1-r} (2E_* - rE) \right] \mathcal{A}^2(E) \delta^{ij}, \end{aligned} \quad (\text{B22a})$$

$$\mathcal{A}_B^{ij}(E) \longrightarrow \left(\frac{g^2}{4m f_\pi^2} \right) \frac{(-2)r^{5/2} \mu^3}{3\pi(d-3)} (E + E_*) \mathcal{A}^2(E) \delta^{ij}. \quad (\text{B22b})$$

- [1] S. K. Choi *et al.* [Belle Collaboration], Phys. Rev. Lett. **91**, 262001 (2003) [hep-ex/0309032].
- [2] S. L. Olsen, Front. Phys. **10**, 101401 (2015) [arXiv:1411.7738].
- [3] R. Aaij *et al.* [LHCb Collaboration], Phys. Rev. Lett. **110**, 222001 (2013) [arXiv:1302.6269].
- [4] E. Braaten and M. Kusunoki, Phys. Rev. D **69**, 074005 (2004) [hep-ph/0311147].
- [5] E. Braaten and H.-W. Hammer, Phys. Rept. **428**, 259 (2006) [cond-mat/0410417].
- [6] S. Fleming, M. Kusunoki, T. Mehen and U. van Kolck, Phys. Rev. D **76**, 034006 (2007) [hep-ph/0703168].
- [7] S. Fleming and T. Mehen, Phys. Rev. D **78**, 094019 (2008) [arXiv:0807.2674].
- [8] S. Fleming and T. Mehen, Phys. Rev. D **85**, 014016 (2012) [arXiv:1110.0265].

- [9] T. Mehen and R. Springer, Phys. Rev. D **83**, 094009 (2011) [arXiv:1101.5175].
- [10] A. Margaryan and R. P. Springer, Phys. Rev. D **88**, no. 1, 014017 (2013) [arXiv:1304.8101].
- [11] M. Jansen, H.-W. Hammer and Y. Jia, Phys. Rev. D **89**, no. 1, 014033 (2014) [arXiv:1310.6937].
- [12] D. L. Canham, H.-W. Hammer and R. P. Springer, Phys. Rev. D **80**, 014009 (2009) [arXiv:0906.1263].
- [13] E. Braaten, H.-W. Hammer and T. Mehen, Phys. Rev. D **82**, 034018 (2010) [arXiv:1005.1688].
- [14] M. H. Alhakami and M. C. Birse, arXiv:1501.06750.
- [15] G. Rosen, Am. J. Phys. **40**, 683 (1972).
- [16] D. B. Kaplan, M. J. Savage and M. B. Wise, Phys. Lett. B **424**, 390 (1998) [nucl-th/9801034].
- [17] J. P. Lees *et al.* [BaBar Collaboration], Phys. Rev. Lett. **111**, no. 11, 111801 (2013) [arXiv:1304.5657].
- [18] S.-K. Choi, S. L. Olsen, K. Trabelsi, I. Adachi, H. Aihara, K. Arinstein, D. M. Asner and T. Aushev *et al.*, Phys. Rev. D **84**, 052004 (2011) [arXiv:1107.0163].